Contract No. Nonr 839(38)

68-23

AD 673953

NEAR WAKE OF A SLENDER CONE AT LARGE ANGLE OF ATTACK

by

E. M. Schmidt and Robert J. Cresci

DDC
RECEIVED
SEP 4 1968
B

JULY 1968

POLYTECHNIC INSTITUTE OF BROOKLYN

DEPARTMENT
of
AEROSPACE ENGINEERING
and
APPLIED MECHANICS

This document has been approved for public release and sale; its distribution is unlimited

PIBAL Report No. 68-23

Reproduced by the
CLEARINGHOUSE
for Federal Scientific & Technical
Information Springfield Va. 22151

50

NEAR WAKE OF A SLENDER CONE AT LARGE ANGLE OF ATTACK

by

E. M. Schmidt and Robert J. Cresci

This research has been conducted under Contract Nonr 839 (38) for PROJECT DEFENDER, and was made possible by the support of the Advanced Research Projects Agency under Order No. 529 through the Office of Naval Research.

Reproduction in whole or in part is permitted for any purpose of the United States Government.

Polytechnic Institute of Brooklyn

Department

of

Aerospace Engineering and Applied Mechanics

July 1968

PIBAL Report No. 68-23

BLANK PAGE

NEAR WAKE OF A SLENDER CONE AT LARGE ANGLE OF ATTACK†

by

E. M. Schmidt* and Robert J. Cresci**

Polytechnic Institute of Brooklyn, Graduate Center

Farmingdale, New York

ABSTRACT

The near wake of a sharp, slender cone at an angle of attack equal to the half-cone angle (10°) is studied experimentally. Tests were run at two different Reynolds numbers; these correspond to (i) completely laminar flow on the surface ($Re_D = 0.15 \times 10^6$) and, (ii) laminar flow on the windward and turbulent on the leeward surface ($Re_D = 0.55 \times 10^6$). The nature of the surface boundary layer was determined by measuring the surface heat transfer over a wide range of test Reynolds numbers ($0.6 \times 10^5 \leq Re_D \leq 1.2 \times 10^6$) and comparing the data with theoretical analyses.

Wake data obtained correspond to radial profiles taken in the plane of symmetry; total temperature, pitot, and static pressures are measured from the rear stagnation point to approximately seven diameters downstream of the base. Centerline distributions of Mach number, stagnation pressure, and static temperature are computed and compared to the corresponding results at zero angle of attack.

---

† This research was supported under Contract Nonr 839(38) for PROJECT DEFENDER, and the Advanced Research Projects Agency under Order No. 529 through the Office of Naval Research.

* Research Associate

** Assistant Director of Gas Dynamics Laboratory

TABLE OF CONTENTS

Section		Page
I	Introduction	1
II	Model Design and Instrumentation	4
III	Presentation and Discussion of Results	6
IV	Concluding Remarks	13
V	References	15

LIST OF ILLUSTRATIONS

Figure		Page
1	Schematic of Test Configuration	17
2	Heat Transfer to Cone Surface ($\bar{s}$ = 2.8)	18
3	Surface Pressure Distribution	19
4	Location of Transition and Fully Turbulent Boundary Layer	20
5	Centerline Distribution of Static Pressure	21
6	Centerline Distribution of Stagnation Temperature	22
7	Centerline Distribution of Mach Number	23
8	Centerline Distribution of Stagnation Pressure	24
9	Centerline Distribution of Static Temperature	25
10	Pitot Pressure Profiles	
	(a) $\bar{x}$ = 1.50	26
	(b) $\bar{x}$ = 2.00	27
	(c) $\bar{x}$ = 2.50	28
	(d) $\bar{x}$ = 3.00	29
	(e) $\bar{x}$ = 3.80	30
	(f) $\bar{x}$ = 4.50	31
11	Shock Configuration	32
12	Static Pressure Profiles	
	(a) $\bar{x}$ = 1.50	33
	(b) $\bar{x}$ = 2.00	34
	(c) $\bar{x}$ = 2.50	35
	(d) $\bar{x}$ = 3.00	36

Figure		Page
13	Stagnation Temperature Profiles	
	(a) $\bar{x} = 1.75$	37
	(b) $\bar{x} = 2.00$	37
	(c) $\bar{x} = 2.50$	38
	(d) $\bar{x} = 3.00$	38
	(e) $\bar{x} = 3.75$	39
	(f) $\bar{x} = 4.50$	39
14	Base Pressure Distribution	40

LIST OF SYMBOLS

C_p	specific heat at constant pressure
D	cone base diameter (8.0 inches)
h	enthalpy
k	coefficient of thermal conductivity
M	Mach number
Nu $\equiv$	$q_w C_{p_\infty} D/k_\infty (h_{s_\infty} - h_w)$ - Nusselt number
p	static pressure
p_t	pitot pressure
p_b	base pressure
q	heat transfer rate
$Re_D \equiv$	$\rho_\infty V_\infty D/\mu_\infty$ - Reynolds number
r	radial coordinate measured from centerline
s	cone surface coordinate
T	temperature
V	velocity
x	coordinate in free stream direction measured from cone base
$(\bar{\ })$	coordinate normalized with respect to base diameter
α	angle of attack
ρ	mass density
μ	coefficient of viscosity
φ	azimuthal angle measured from windward axis

Subscripts

s	stagnation conditions
w	conditions evaluated at cone surface
∞	free stream conditions

1	local conditions
2	conditions behind a normal shock

SECTION I

INTRODUCTION

The near wake of blunt-based slender bodies represents a fundamental fluid mechanical problem which derives its basic features from the formation of the separated flow regime. The necessity of studying this region in detail has been dictated by the effect of the local flow field properties on communications with, guidance of, and identification of high speed vehicles. A comprehensive review of the available literature connected with this problem is presented in reference (1) while the current development of theoretical analyses of the near wake region is typified by the results of references(2) through (4). These analyses are applicable to two dimensional bodies with laminar boundary layers. Even in this somewhat limited context, moreover, there arise certain difficulties which restrict the solutions to limited ranges in free stream Reynolds numbers and Mach numbers, cf. reference (4). For the more practically interesting problem of an axisymmetric body with either a laminar or turbulent boundary layer, the inherent complexity of analyzing such a region is even greater, therefore, no analysis is currently capable of accurately predicting the near wake properties for such a configuration.

Certain properties of the base flow region are significant from the viewpoint of design and advanced development of reentry bodies, e.g. the temperature of the fluid in the recirculating region, and near wake velocity profiles, which are necessary initial conditions for far-wake computations. Since theoretical analyses for the prediction of these properties are not yet available, attempts have been made to correlate information of this type in terms of the free stream conditions and vehicle configurations from experimental data, cf. references (5) through (7). It has therefore become necessary to obtain a large amount of experimental data

for this purpose; this data also provides information for comparison with proposed theoretical analyses, and indicates the basic flow pattern from which the theoretician can gain insight into mechanisms governing the flow in this region. The experimental data has been obtained by various techniques including ballistic range firings, shock tunnels, and blowdown wind tunnels. A summary of the experimental reports issued over the past several years has been presented in reference (8) and includes near wake data for a variety of vehicle configurations, free stream Mach numbers, Reynolds numbers, wall temperature ratios, etc. Although there is a reasonably large amount of data available, certain aspects of the flow pattern have not yet been satisfactorily resolved and require further investigation.

A configuration which has received little attention as yet is the axisymmetric body, or slender body at angle of attack. This problem is of extreme practical importance since a re-entering hypersonic vehicle will not necessarily be at zero attitude throughout its entire flight trajectory. In fact, if maneuvers are desired, the angle of attack required to produce the necessary lateral forces can be quite large. Even without this consideration, however, oscillations of the vehicle about the zero angle of attack attitude are possible and may have a significant influence on the general behavior of the base flow. This can also be important in interpretating data obtained from free flight firings, (either in ballistic ranges or in the atmosphere) since, under these conditions the zero attitude configuration may be difficult to achieve and even more difficult to measure accurately. Some wind tunnel data is currently available concerning this phenomenon and has been presented in reference (9). It consists of a 10° half angle cone tested at $M_{\infty} = 6.0$ and at a 10° angle of attack. The free stream Reynolds number is sufficiently large so that fully turbulent flow is achieved both on the cone surface and in the

near wake. The corresponding data for $\alpha = 0^{o}$ are presented in reference (6). Significant differences in the flow field were observed due to the angle of attack of the body, in particular, the stagnation pressure recovery in the near wake was significantly increased.

It is known that the behavior of the near wake of an axisymmetric body is directly related to the nature of the surface boundary layer at the model shoulder, therefore, for the angle of attack configuration it is of considered importance to determine whether a change of vehicle attitude can sufficiently alter the surface boundary layer characteristics and the corresponding base flow to change the near wake from a laminar to a turbulent condition. In other words, if the free stream Reynolds number is sufficiently low so that both the surface boundary layer and the near wake are laminar at $\alpha = 0^{o}$, and then a change in attitude occurs, the question arises as to whether the altered nature of the boundary layer on the surface of the body can significantly alter the mixing processes occuring in the near wake.

It is the purpose of this investigation, therefore, to examine the flow characteristics in the near wake of a slender body at angle of attack for reasonably low Reynolds numbers. A detailed study of the surface properties on the cone is performed both at zero and non-zero angle of attack to accurately ascertain the nature of the boundary layer under these conditions. This is necessary if a more complete understanding of the measured wake data is to be obtained. The flow field is surveyed between the base and several base diameters downstream of a sharp, 10° half angle cone which is wire supported at a 10° angle of attack. Tests were conducted at a free stream Mach number of 7.7 in the PIBAL hypersonic facility at two free stream Reynolds numbers; these are 0.15×10^{6} and 0.55×10^{6} based on model diameter. The average stagnation temperature was $1700^{o}R$ producing a wall to stagnation temperature ratio of 0.32. The same model

was also tested previously at zero inclination, cf. reference (10), thus, a comparison of results is performed between the zero and non-zero angle of attack configurations.

SECTION II

MODEL DESIGN AND INSTRUMENTATION

The model, illustrated schematically in figure (1), is a 10° half angle cone which was rolled and machined to 0.05 inches thickness from a stainless steel sheet. The surface is instrumented for local heat transfer and static pressure measurements; for these tests, the model is supported by a base sting to facilitate removal of the instrumentation leads from the wind tunnel. Heat transfer gauges, which are located at various positions along a generator of the cone, consist of fine thermocouple wires spot welded to the inside of the model skin. The local heat transfer rate is calculated by the thin skin technique, utilizing the basic assumption that no heat is transferred along the cone surface, and that the inner surface is adiabatic. Static pressure taps are also located along a conical ray, the peripheral distribution of surface pressure being obtained by rotating the model about its axis on the model mount.

To obtain data in the near wake, the model is supported by six braided cables of 0.03 inches diameter; three of these support the model at the nose and three just slightly aft of the model center of gravity. In this manner, the rear wires penetrate the model boundary layer at a location of more than 250 wire diameters upstream of the model base. This is done to assure no wire interference effects on the base region, since in this distance the major influence

of the wires has been dissipated.

The wake survey data obtained correspond to radial variations of flow parameters in the model plane of symmetry at selected axial positions. These measurements of local values of the pitot and static pressures and stagnation temperature are obtained only in the supersonic portion of the near wake region. The total pressure rake consists of standard pitot tubes with blunt leading edges connected to Statham 0.5, 2.5, and 15 lb./in.^{2} transducers. The static probes consist of tubes with six static holes drilled around their periphery at a distance of 15 tube diameters from the tip; slender (5°) cones are installed at the tips of the probes to facilitate the decay of local static pressure on the probe surface to that of the local free stream. The static pressure is measured using Hastings DV - 13 thermocouple type gauges. From the pitot and static pressure data, the local Mach number is obtained and the corresponding value of the local stagnation pressure can then be computed. The stagnation temperature probes are open-tip, bare wire thermocouples stretched across two support struts. The stagnation temperature together with the Mach number obtained from the pressure survey allows the calculation of local static temperature.

The tests were performed at Mach 7.7 with air as the test gas. The duration of sustained hypersonic flow in this tunnel is on the order of 30 seconds, however, to obtain wake data at a relatively constant value of the wall temperature ratio, a run length of about 5 seconds is used. This is sufficient to achieve a stabilization of the pressure instrumentation and still have a relatively uniform model surface temperature. The tunnel stagnation pressure was varied from 30 psia to 550 psia to obtain the desired variation in Reynolds number necessary to compare with the theoretical analyses of the boundary layer and to determine whether the boundary layer is laminar or turbulent. The complete wake survey

at $\alpha = 10^{\circ}$ was conducted at nominal tunnel stagnation pressures of 75 and 275 lb./in.^{2} and roughly 1700°R stagnation temperature, which corresponds to free stream Reynolds numbers of 0.225×10^6 and 0.825×10^6 per ft., respectively.

SECTION III

PRESENTATION AND DISCUSSION OF RESULTS

One method which has been utilized extensively in the past to ascertain the nature of the boundary layer characteristics on a surface is to measure the local heat transfer rate and compare this to theoretical analyses; this is particularly useful where, as in the present tests, the boundary layer thickness is too small for standard pressure probing techniques. The surface heat rates therefore, have been obtained for the test model at both zero and non-zero angles of attack and typical results are shown in figure (2). The data is presented in terms of a Nusselt number versus a Reynolds number based on free stream conditions and the base diameter of the cone. This particular variation of heat transfer corresponds to a surface location ($\bar{s} = 2.80$) on the cone which is close to the shoulder ($\bar{s}_b = 2.88$). Figure (2a) presents the data for the zero angle of attack condition and includes the laminar boundary layer predictions of reference (11) and the fully turbulent theory of reference (12). It is observed that by varying the stagnation pressure of the tunnel, a complete range of boundary layer behavior can be obtained corresponding to either completely laminar, transitional, or fully turbulent at the shoulder. For Reynolds numbers less than 0.65×10^6, the boundary layer is seen to be laminar over the entire cone surface.

For the angle of attack configuration, the corresponding data for the same

surface location is presented in various meridian planes in figures (2b) and (2c). The angle φ is measured from the windward plane and for $\varphi = 0$, the theoretical laminar boundary layer analysis of reference (13) is also included. It is evident from this comparison that the boundary layer is laminar in this plane over the entire test Reynolds number range. The corresponding data and analysis is also shown in the cross plane ($\varphi = 90^{\circ}$) and again it is observed that the boundary layer is laminar. Figure (2c) presents the heat transfer data on the cone surface in the leeward plane. In this case, there is no theoretical analysis available since the cross flow is toward the plane of symmetry and the inviscid flow field is not accurately known. In fact, the analysis of reference (14) indicates (for lower Mach numbers) that the flow will separate along a generator of the cone when the angle of attack is approximately equal to the semi-vertex cone angle. This analysis, however, is based on the assumption of isentropic flow throughout the flow field. For the present case the free stream Mach number is sufficiently large and the semi-vertex cone angle is high enough so that the results of reference (14) are not applicable, in addition, the inviscid flow field around the cone is not accurately known in the present case. In order to determine, therefore, whether the flow has separated or not, the static pressure distribution around the periphery of the cone was measured. These results are shown in figure (3), where the local surface pressure, normalized with respect to the free stream static pressure, is presented as a function of the peripheral angle. Data are shown for both the low and high Reynolds number condition, i.e., at Reynolds numbers equal to 0.15×10^6 and 0.55×10^6 respectively. It appears that no separation is present under either test condition since the pressure is monotonically decreasing from the windward to the leeward plane around the cone; therefore, the surface heat transfer in the leeward plane can be examined to de-

termine the nature of the surface boundary layer. For comparison purposes, a flat plate theory is applied using the undisturbed free stream conditions as the inviscid flow. The results of these analyses are plotted in figure (2c) for the laminar and turbulent conditions corresponding to the experimental heat transfer data. Although the quantitative agreement is not good, the qualitative behavior of the heat transfer as a function of Reynolds number is quite clear. A region of laminar flow is seen to occur at low Reynolds numbers followed by transitional and then a fully turbulent boundary layer. In all cases, the Reynolds number at which transition occurs and the Reynolds number at which a fully turbulent condition exists can be determined quite accurately from these plots. Similar data has been obtained in other planes to determine the lateral extent of transitional flow on the leeward surface; these correspond to values of $\phi = 135^{\circ}$, and 160°. The data are not shown here but the results are summarized in figure (4) where the transition Reynolds number and the fully turbulent Reynolds number are plotted as a function of peripheral angle around the cone; also included are the corresponding points for the zero angle of attack configuration.

For the cone at angle of attack it is seen that transition is initiated at a considerably lower Reynolds number than for the zero angle of attack condition in the leeward plane. It is also observed (cf. figure 4) that the transitional region occurs over a small area in the vicinity of the leeward plane; for the remainder of the model surface, the flow is completely laminar even at the highest Reynolds numbers attainable in the PIB tunnel. As noted previously, the wake surveys were performed at Reynolds numbers of 0.15×10^6 and 0.55×10^6. From figure (4) it can be seen that these particular Reynolds numbers correspond in one case to a completely laminar flow over the surface and,

in the other, to a surface boundary layer which is laminar, transitional, or turbulent, depending on the peripheral location.

Since the near wake characteristics of axisymmetric bodies have been found to be strongly dependent on the surface boundary layer at the model shoulder, it is of interest to determine the wake flow field conditions that are produced for the present configuration at different Reynolds numbers. With this in mind the centerline variation of local properties such as Mach number, temperature, and pressure will be examined for the angle of attack condition and compared to the corresponding zero inclination data of reference (10).

The static pressure distribution along the model centerline is shown in figure (5) for both laminar and turbulent flow on the model surface for the zero inclination and 10° angle of attack conditions. Within the experimental accuracy, there is little observable difference in the data for the various conditions. The static pressure is seen to reach a pressure somewhat higher than free stream and then it decays to the free stream value roughly four model diameters downstream of the base. It should be noted that although the data presented in figures (5) through (9) correspond to the geometric centerline distribution for the zero angle of attack configuration, when the cone is inclined at an angle with the free stream this centerline does not correspond to the "local symmetry axis." Therefore, the angle of attack data correspond to the maximum local static, or minimum local pitot pressures and total temperatures rather than the values obtained along the geometric centerline. These occur slightly off axis as can be seen in figures (10), (12), and (13).

The total temperature variation along the centerline is shown in figure (6). The turbulent zero angle of attack data is seen to recover to the free stream temperature more rapidly at first than the corresponding laminar flow data. How-

ever, at angle of attack, there appears to be only a small difference between the data obtained at the two different Reynolds numbers. Figure (7) presents the centerline variation of Mach number obtained from the various sets of experimental pitot and static pressure measurements available. Again, for the zero inclination model, the Mach number recovers more rapidly for the turbulent condition. Further downstream, it appears that the low Reynolds number flow is transitional and the differences between the two are significantly decreased. The angle of attack condition moreover produces a higher local Mach number initially than even the fully turbulent zero angle data; this occurs even for the low Reynolds number case where the surface boundary layer is completely laminar.

Since these two configurations produce similar static pressure distributions, it is evident that the stagnation pressure recovery in the near wake will be changed due to the difference in Mach number variation. This can be seen in figure (8) which presents the variation of local stagnation pressure (normalized with respect to the free stream stagnation pressure) along the axis. Again, it is seen that the recovery to the free stream condition occurs more rapidly at angle of attack than for the zero angle of attack case with a fully turbulent boundary layer. The recovery of the near wake flow parameters thus appears to be influenced by two different phenomena in the angle of attack configuration. First, the angle of attack produces a localized region on the cone surface wherein the boundary layer which was originally laminar has become transitional or turbulent at lower Reynolds numbers than expected for the zero inclination case. This effects the mixing processes and therefore the behavior of the local flow conditions in the wake. In addition, it appears that for the angle of attack configuration there is a large scale mixing caused by the vortical inviscid flow over the cone surface which further increases the pressure recovery in the wake and thus, it approaches its free stream value

more rapidly.

From the Mach number and total temperature data, the static temperature along the centerline is computed and shown in figure (9). The overall trends observed in the other flow parameters are also seen to occur in the temperature behavior, although in this case, they are even more evident. In particular, the high Reynolds number angle of attack tests produce extremely rapid recovery to the free stream temperature; there is a significant difference between this data and even the fully turbulent, zero angle data. Even more important is the behavior close to the base region where the static temperature is between 20% to 50% lower when the cone is at angle of attack in comparison to the zero angle condition.

Pitot pressure profiles are presented in figures (10a) through (10f). The trailing shock shape can be roughly determined from the observed discontinuity in the pitot profiles; this is shown to scale in figure (11), with the corresponding zero angle of attack shock shape as determined from Reference (10). As noted previously, the symmetry axis in the viscous core is displaced toward the leeward side of the cone by an initial amount approximately equal to one tenth of the base diameter. As the distance downstream of the base increases, this radial shift decreases until it is essentially zero ($\bar{x} = 4.5$). The trailing shock shape is also displaced in the same direction although it is seen to require a significantly longer distance to approach the axisymmetric shock configuration.

In order to determine the range of validity of the measured profiles, the conical shock and base expansion fan are also sketched in figure (11). Reflection of the bow shock from the tunnel wall (or the displacement thickness as an approximate wall correction) on the windward side of the model indicates an approximate intersection with the trailing shock between four and five base diameters downstream of the model. Although additional radial surveys were obtained for

values of $\bar{x}$ up to 7.5, these are not included since the data is of questionable validity outside of the trailing shock radius. Centerline conditions, however, are expected to be reasonable for distances up to seven base diameters down stream of the model. The disturbance from the leeward surface of the cone is seen to have no effect on the measured flow variables for considerably larger distances.

The static pressure profiles are shown in figures (12a) through (12f). In these plots, the shock location is also evident although its location is not as accurate since the pressure readings on the static probes are affected for some distance on either side of the exact shock impingement location. In addition, the off-axis data for small downstream distances incur a larger percentage error than the pitot pressures due to the possibility of local flow inclination. Total temperature profiles are presented in figures (13a) through (13f) and exhibit the same general behavior as the pressure plots in relation to the off axis location of the minimum temperatures. One major difference is that all the temperature variation is concentrated within one base diameter of the centerline whereas the pressure field is disturbed to a much larger lateral extent.

Figure (14) presents the radial distributions of base pressure corresponding to the various test conditions previously discussed. The angle of attack tests produce a large decrease in the level of the base pressure in comparison to the data corresponding to zero angle of attack; this is observed even for the low Reynolds number tests. In addition, there is an extremely large variation in pressure along the base surface, with the lower pressure occuring adjacent to the windward plane; it may be noted that at the present test Reynolds numbers, the corresponding base pressure distribution is quite uniform for $\alpha = 0^{\circ}$.

SECTION IV

CONCLUDING REMARKS

In addition to providing some profiles of pitot and static pressure and total temperature in the near wake of a cone at angle of attack, some overall effects of the recovery of the flow variables to their free stream values have been observed. The tests were performed at Reynolds numbers chosen to provide a completely laminar flow over the cone surface in one case so that the effects of large scale "inviscid" mixing could be studied by comparison with laminar cone data at zero angle. The second test Reynolds number was sufficiently large to produce a small region of transitional and fully turbulent flow on the model surface in the leeward plane. Again, comparison of this data with fully turbulent data at zero angle of attack gives some indication of the relative importance of the boundary layer vs. the outer vortical layer in the determination of the wake characteristics. These results can be summarized as follows:

1. Very little difference is observed in the static pressure distribution for the various test configurations, except that the peak over pressure occurs closer to the base with angle of attack. This is consistent with the measured base pressure behavior, since lower base pressures result at angle of attack.

2. Both the static temperature and stagnation pressure data indicate that the inviscid vortical flow dominates the wake characteristics at angle of attack in the immediate base region ($\bar{x} \leq 3$); here, the effect of an initially laminar vs. turbulent boundary layer appears to have little influence on the recovery of these flow parameters. For example, the stagnation pressure for both test conditions at angle of attack are close to each other but higher than would exist at zero angle even for a fully turbulent wake.

However, for larger distances downstream ($\bar{x} > 3$), the angle of attack data for a laminar boundary layer approaches the zero inclination data while that corresponding to an initial turbulent region on the cone surface continues to recover to the free stream conditions very rapidly. At $\bar{x} = 6$, for example, the (laminar) stagnation pressure recovery is roughly 0.03 for both $\alpha = 0^{\circ}$ and $\alpha = 10^{\circ}$; the high Reynolds number (turbulent) data on the other hand, yield values of 0.05 for $\alpha = 0^{\circ}$ and 0.20 for $\alpha = 10^{\circ}$ indicating much more rapid mixing for the latter condition. This may be caused by the eventual spreading of the initial turbulent burst, on the cone surface, throughout the entire viscous region as the distance downstream is increased.

3. Examination of the total temperature profiles, and the trailing shock location indicates that close to the base there is a significant change in total temperature for radial distances larger than the shock radius. This is caused by the three dimensional mixing of the surface boundary layer with the outer flow; the corresponding data at zero angle of attack (ref. 10) shows the viscous core to be the only region where the total temperature is different from its free stream value. Again, this shows the dominance of the vortical outer flow behavior on the flow in the near wake, for the angle of attack configuration.

In summary, both the free stream Reynolds number and the outer vortical flow appear to be significant in the determining the local flow properties in the asymmetric near wake region. Probably even more important than this, in terms of interpretation of flow observables, is the complete change in the near wake behavior (at the same free stream Reynolds number) between the zero and non-zero angle of attack configurations.

SECTION V

REFERENCES

1. Lykoudis, P. S.: A Review of Hypersonic Wake Studies. AIAA Journal, Vol. 4, No. 4, April 1966, p. 577-590.
2. Golick, R. J., Webb, W. H., Lees, L.: Further Results of Viscous Interaction Theory for the Laminar Supersonic Near Wake. AIAA Paper No. 67-61, January 1967.
3. Webb, W. H., Golik, R. J., Vogenitz, R. W., Lees, L.: A Multimoment Integral Theory for the Laminar Supersonic Near Wake. Proceedings of the Heat Transfer and Fluid Mechanics Institute, 1965, p. 168-189.
4. Weiss, R. F.: A New Theoretical Solution of the Laminar, Hypersonic Near Wake. AIAA Paper No. 67-63, January 1967.
5. Zakkay, V., Cresci, R. J.: An Experimental Investigation of the Near Wake of a Slender Cone at $M_\infty = 8$ and 12. AIAA Journal, Vol. 4, No. 1, January 1966, p. 41-46.
6. Martellucci, A., Trucco, H.: Measurements of the Turbulent Near Wake of a Cone at Mach 6. AIAA Journal, Vol. 4, No. 3, March 1966, p. 385-391.
7. Muntz, E. P., Softley, E. J.: A Study of Laminar Near Wakes. AIAA Journal, Vol. 4, No. 6, June 1966, p. 961-968.
8. Waldbusser, E. J.: Hypersonic Laminar Near Wakes. General Electric Document No. 68SD274, June, 1968.
9. Schlesinger, A. J., Martellucci, A.: Wind Tunnel Investigation of the Near Wake of a Cone at Angle of Attack. General Applied Science Labs., Inc., GASL TR No. 581, March 1966.

10. Schmidt, E. M., Cresci, R. J.: An Experimental Investigation of Hypersonic Flow Around a Slender Cone. Polytechnic Institute of Brooklyn, PIBAL Report No. 1031, AD 666117, October 1967.

11. Eckert, E. R. G.: Engineering Relation for Friction and Heat Transfer to Surface in High Velocity Flow. Journal of the Aeronautical Sciences, Vol. 22, 1955, p. 585-586.

12. Cresci, R. J., MacKenzie, D. A., Libby, P. A.: An Investigation of Laminar, Transitional, and Turbulent Heat Transfer on Blunt-Nosed Bodies in Hypersonic Flow. Journal of the Aero/Space Sciences, Vol. 27, No. 6, June 1960, p. 402-414.

13. Reshotko, E.: Laminar Boundary Layer with Heat Transfer on a Cone at Angle of Attack in a Supersonic Stream. NACA TN 4152, December 1957.

14. Moore, Franklin K.: Laminar Boundary Layer On Cone In Supersonic Flow At Large Angle Of Attack. NACA Rept. 1132. 1953.

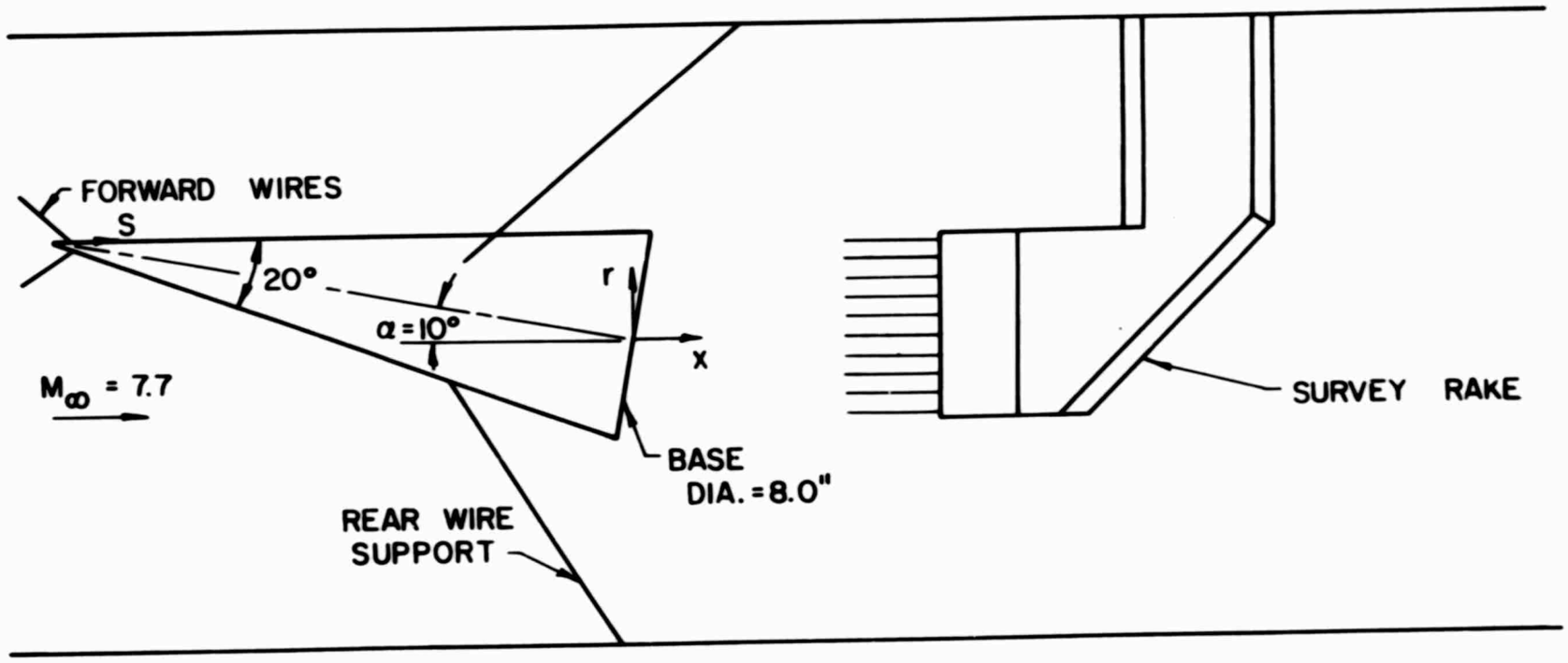

FIG. (1) SCHEMATIC OF TEST CONFIGURATION

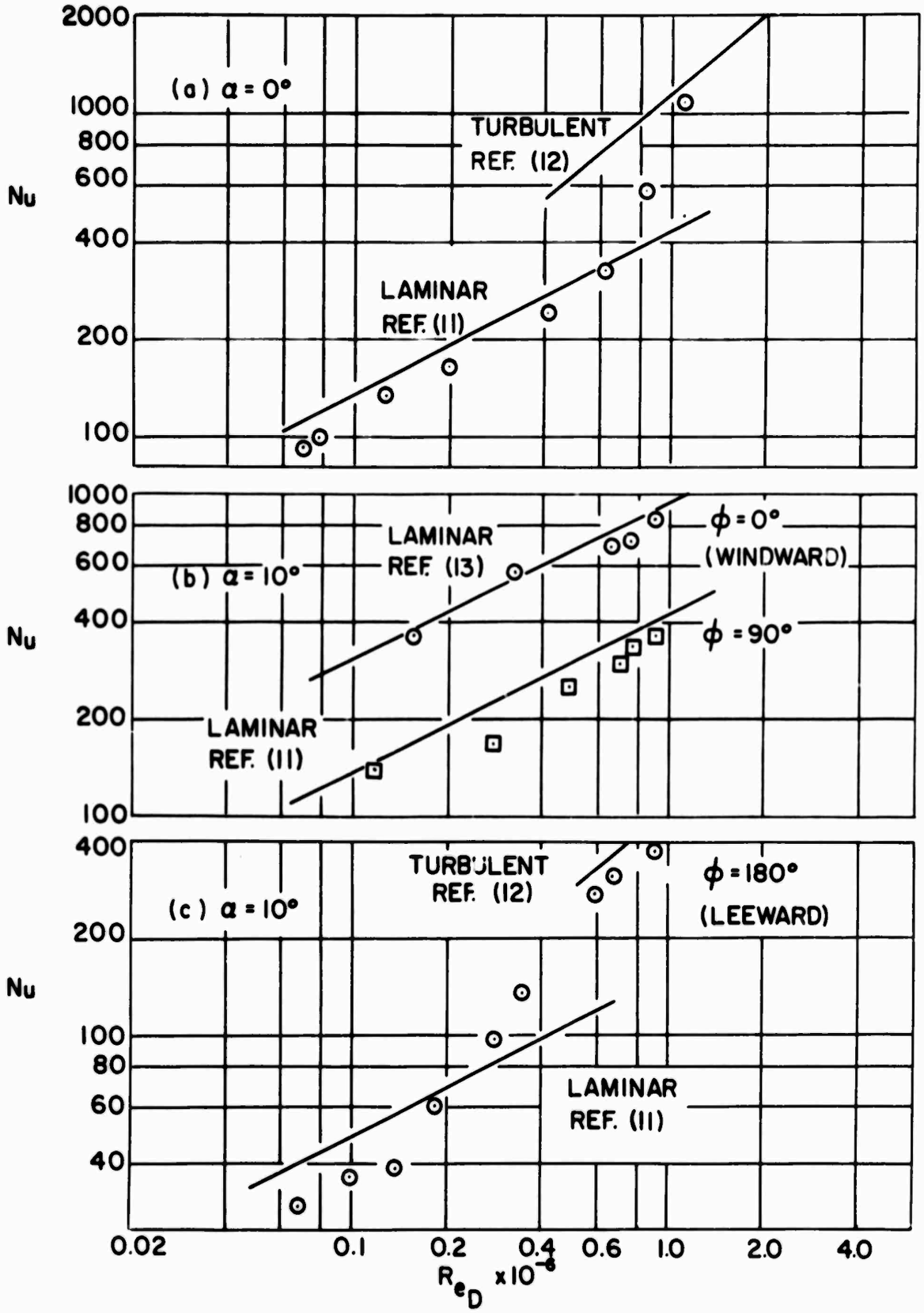

FIG. (2) HEAT TRANSFER TO CONE SURFACE ($\bar{S}$ = 2.8)

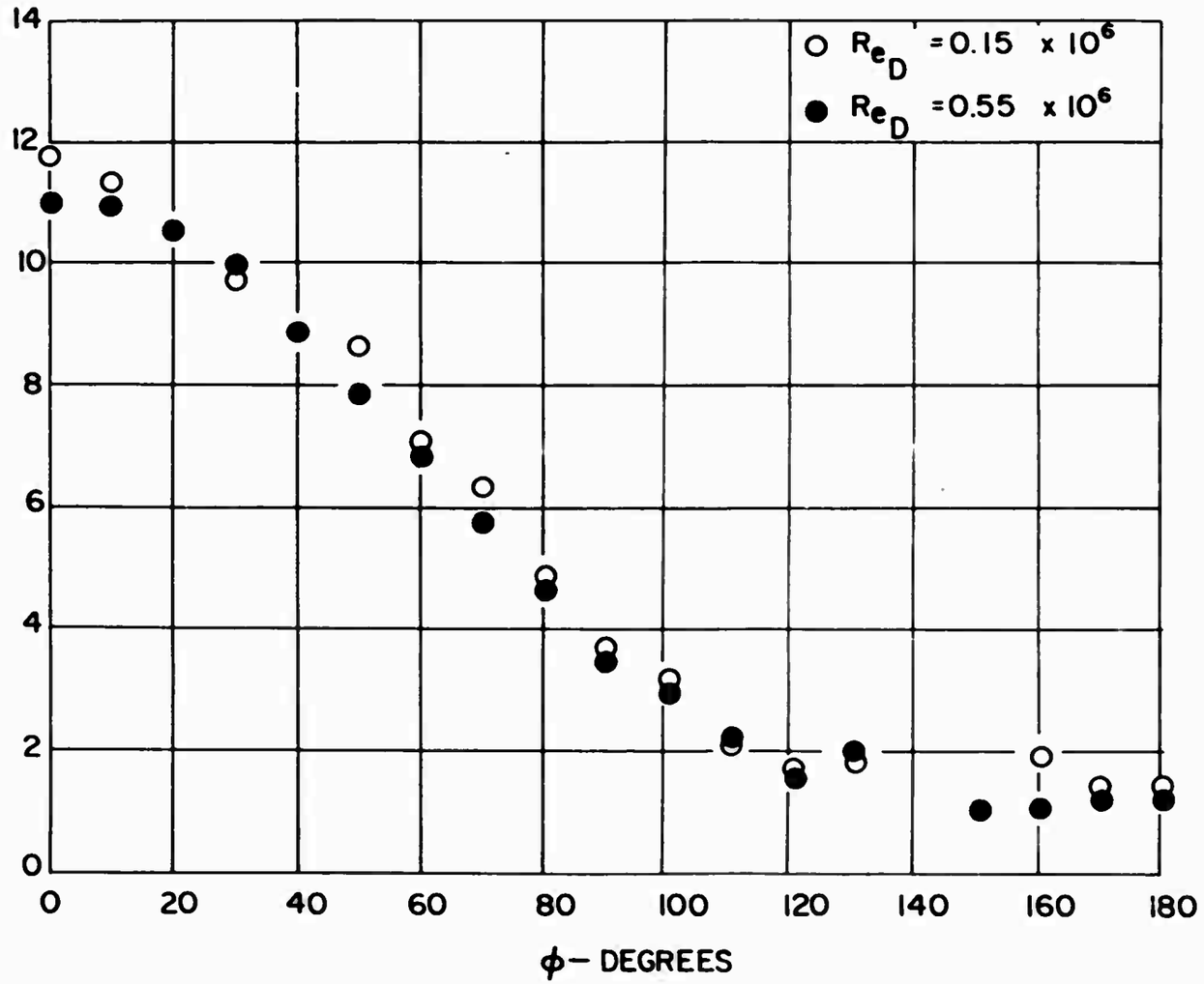

FIG. (3) SURFACE PRESSURE DISTRIBUTION

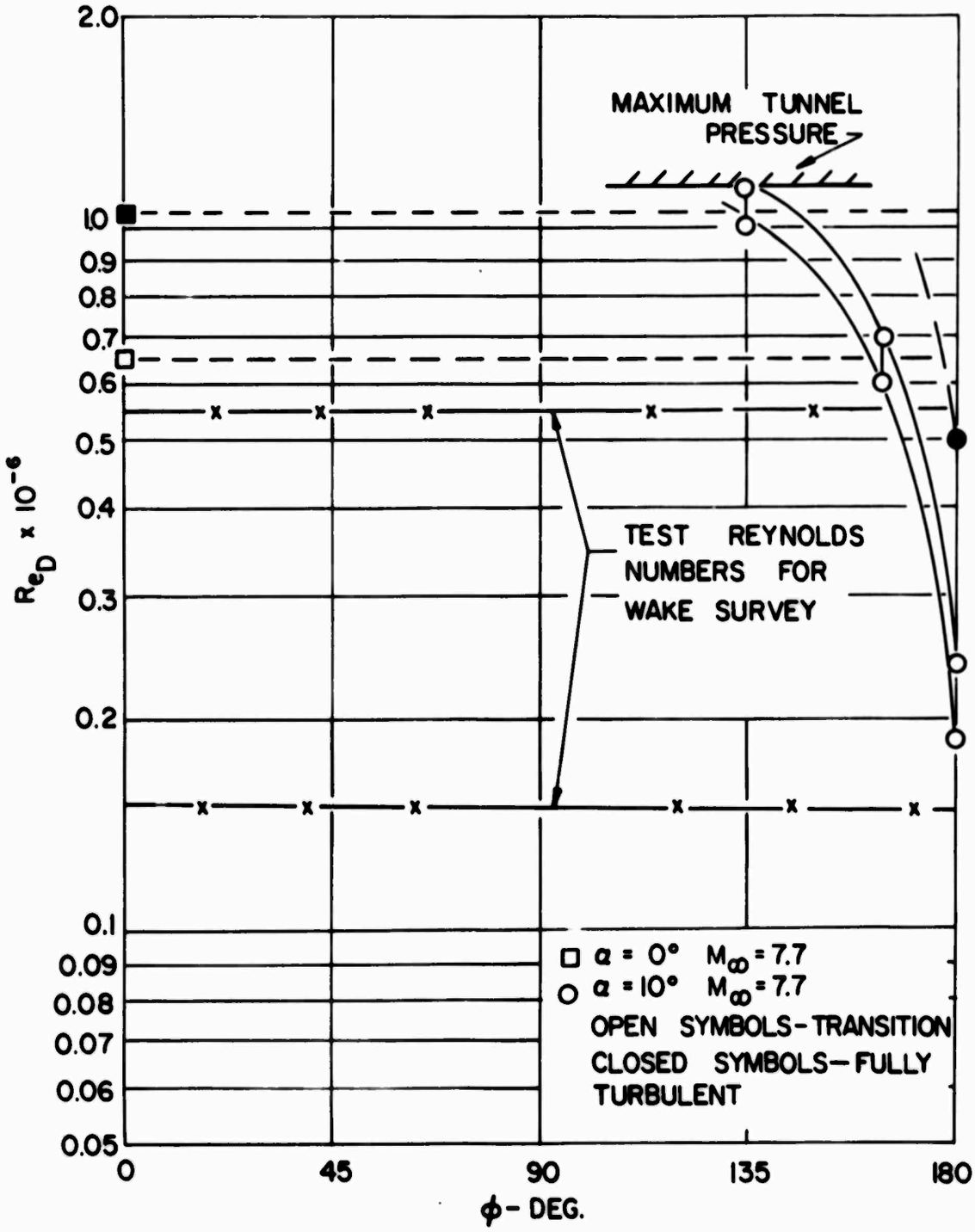

FIG. (4) LOCATION OF TRANSITION AND FULLY TURBULENT BOUNDARY LAYER

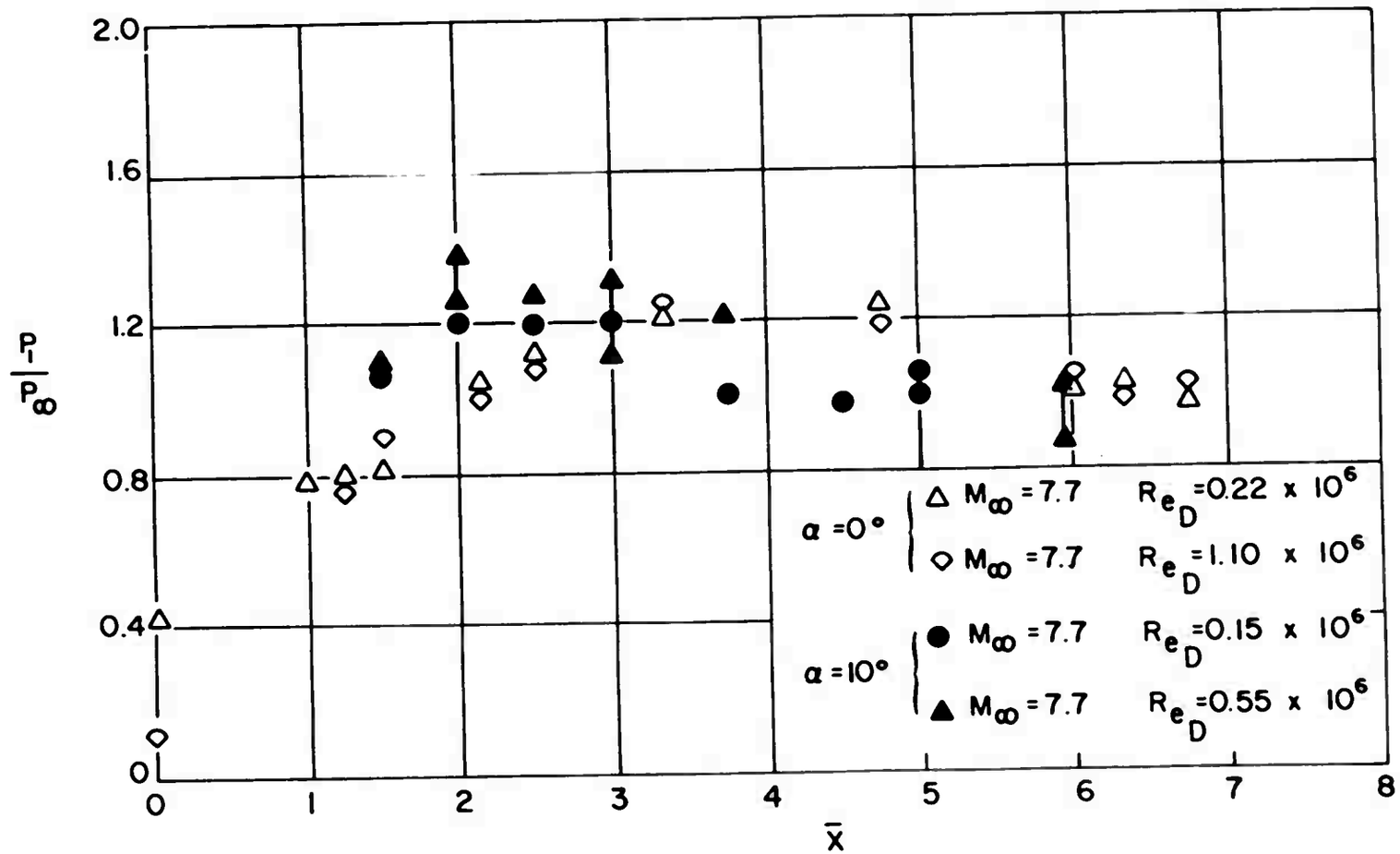

FIG. (5) CENTERLINE DISTRIBUTION OF STATIC PRESSURE

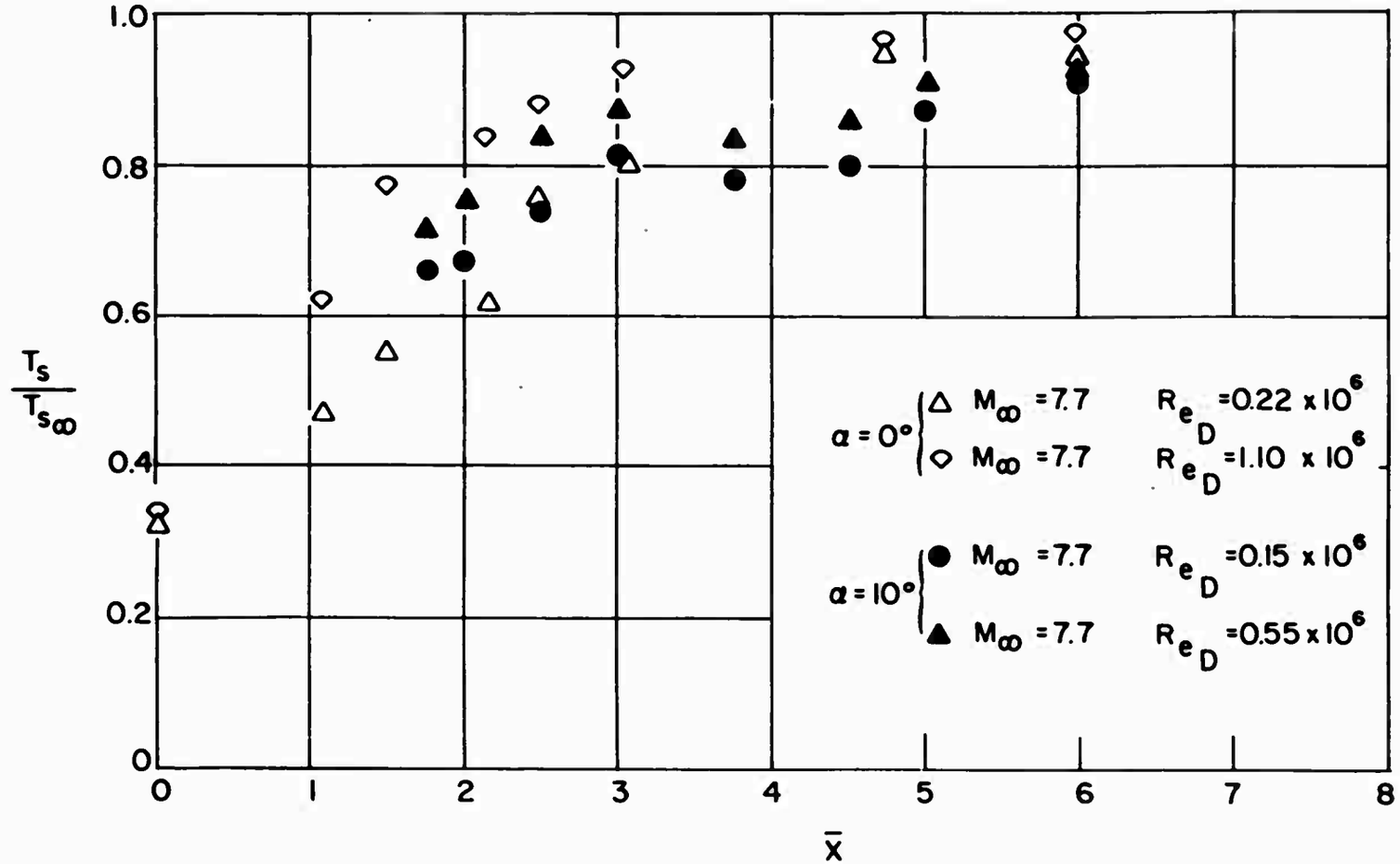

FIG. (6) CENTERLINE DISTRIBUTION OF STAGNATION TEMPERATURE

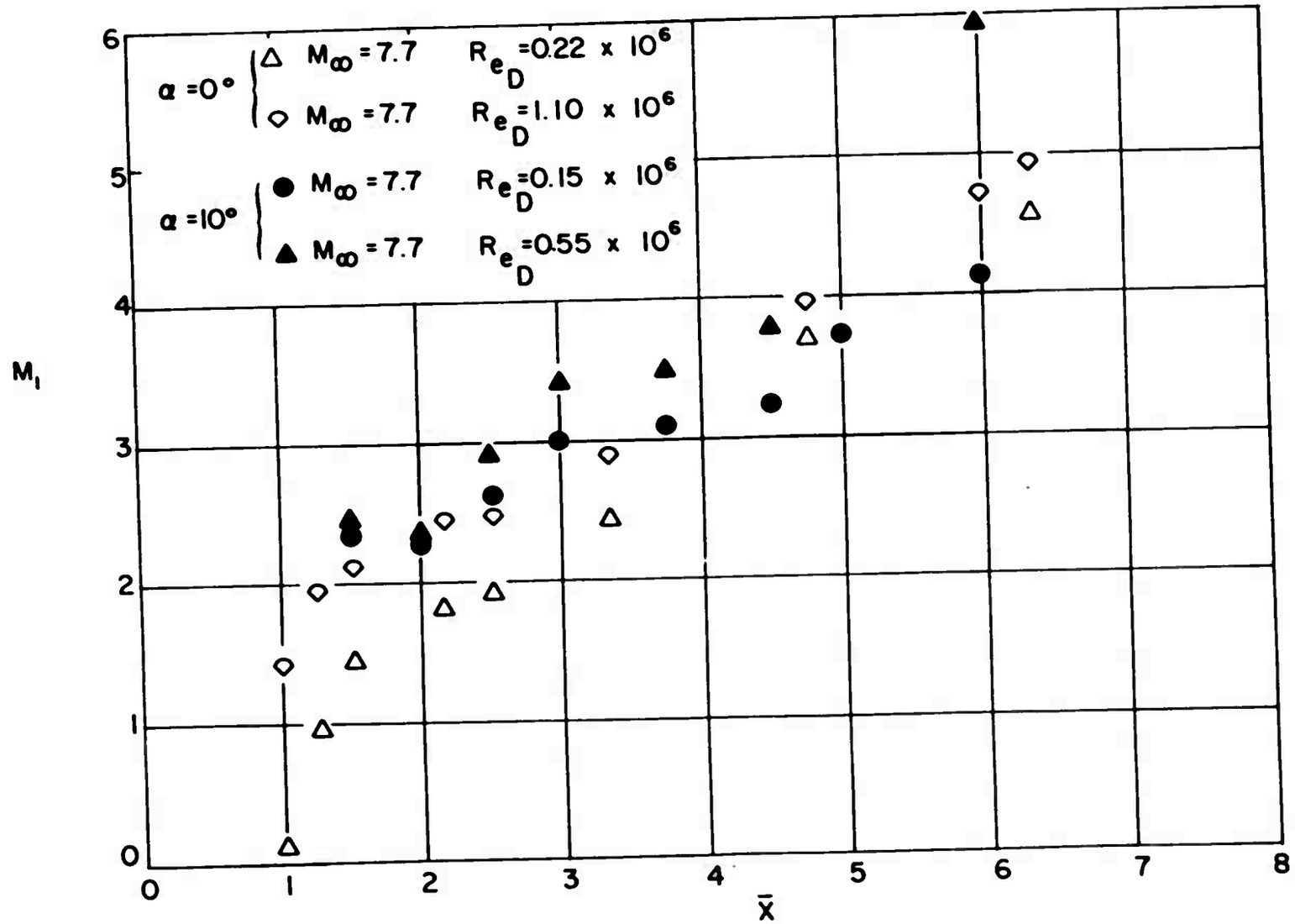

FIG. (7) CENTERLINE DISTRIBUTION OF MACH NUMBER

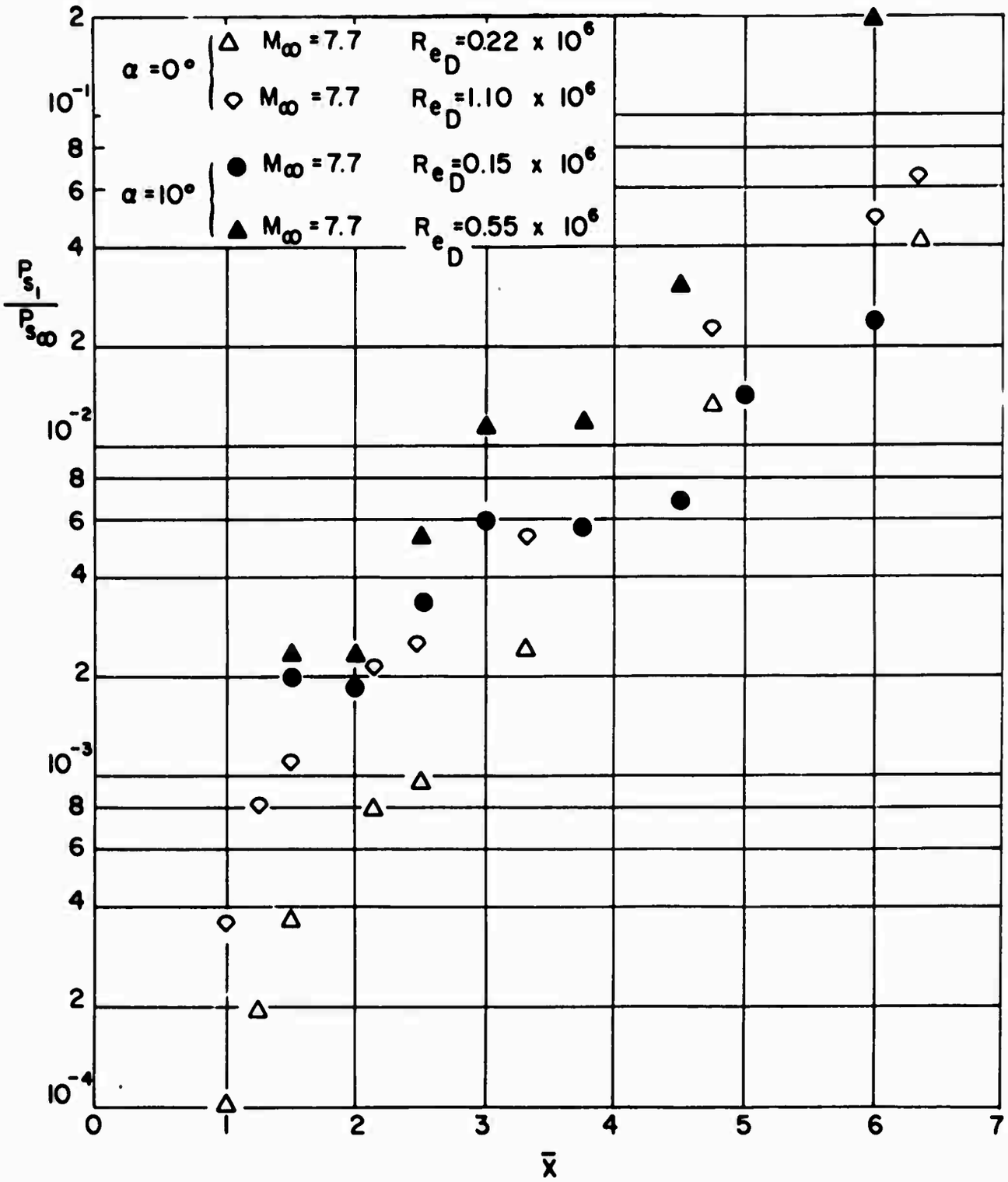

FIG. (8) CENTERLINE DISTRIBUTION OF STAGNATION PRESSURE

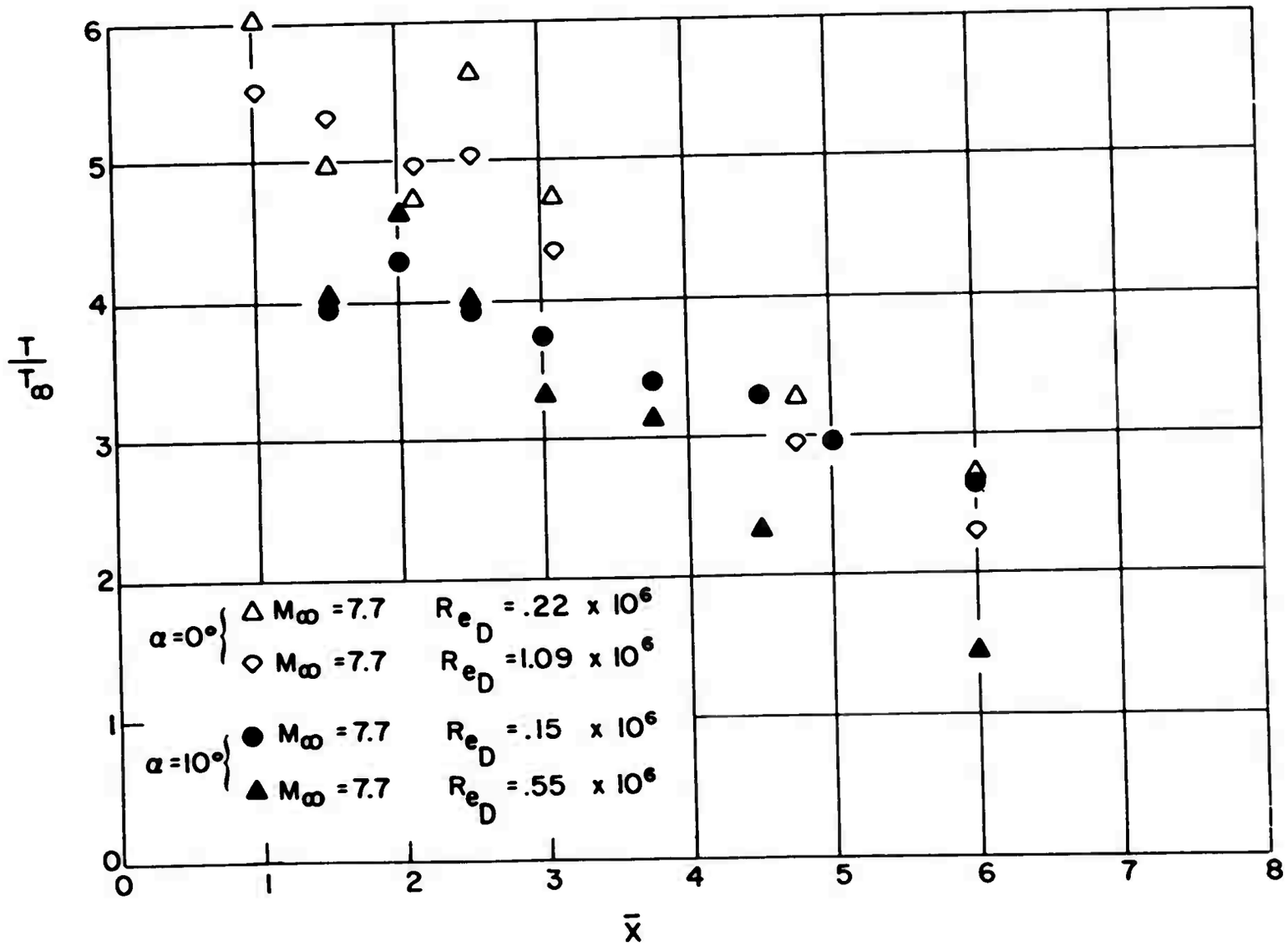

FIG. (9) CENTERLINE DISTRIBUTION OF STATIC TEMPERATURE

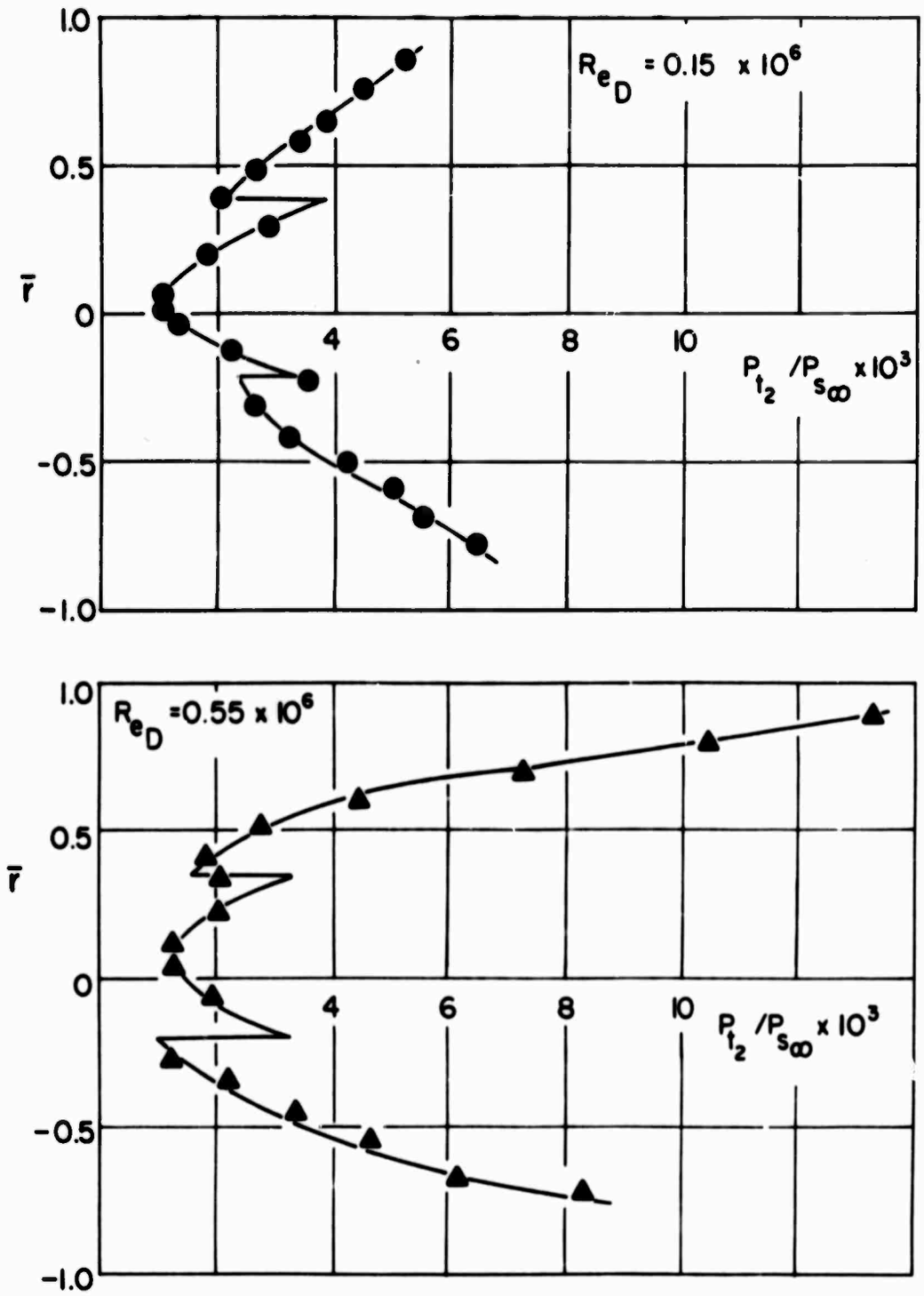

FIG.(10) PITOT PRESSURE PROFILES
(a) $\bar{X}$ = 1.50

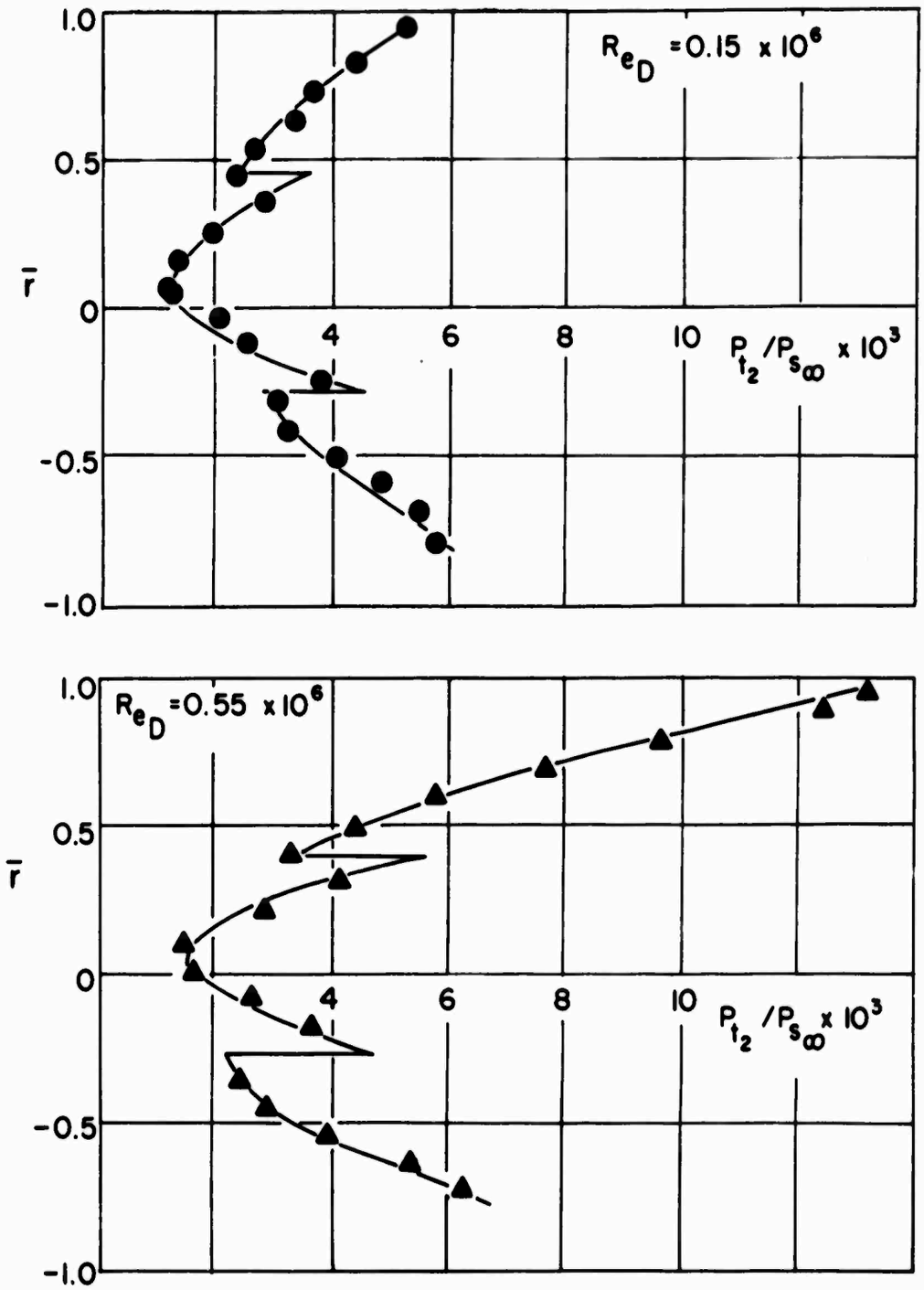

FIG. (10) PITOT PRESSURE PROFILES
(b) $\bar{X}$ = 2.00

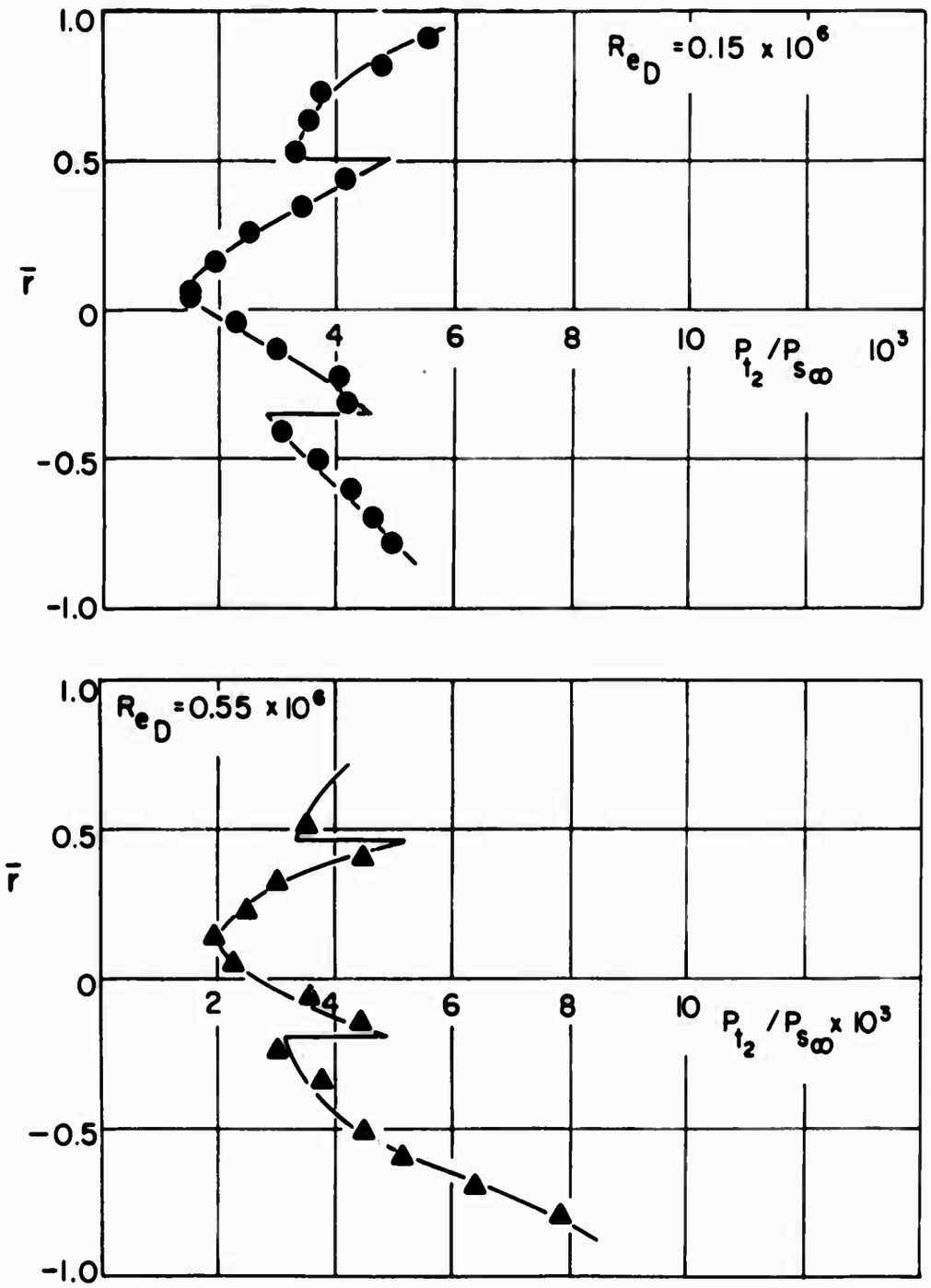

FIG. (10) PITOT PRESSURE PROFILES
(c) $\bar{X}$ = 2.50

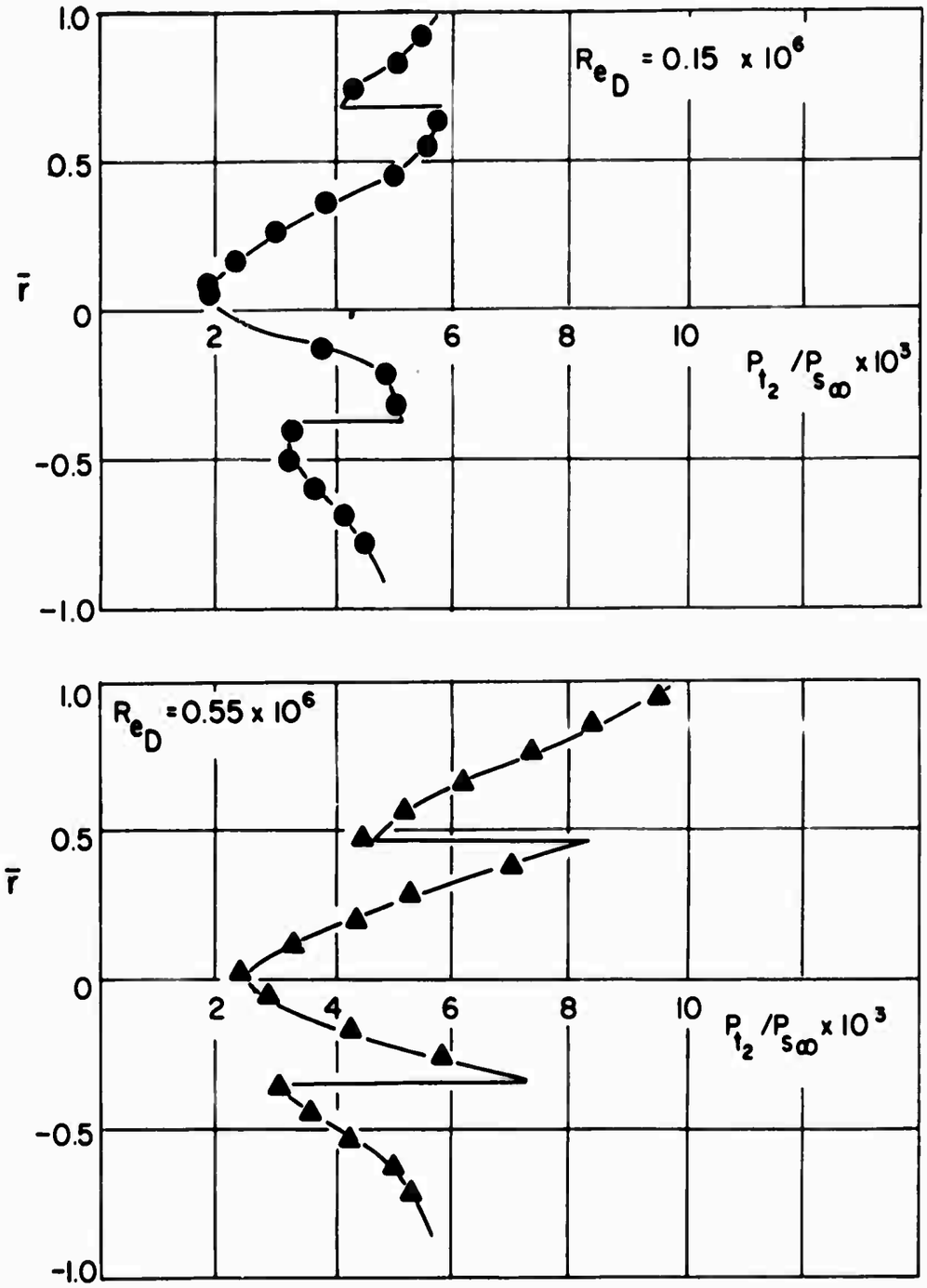

FIG.(10) PITOT PRESSURE PROFILES
(d) $\bar{X}$ = 3.00

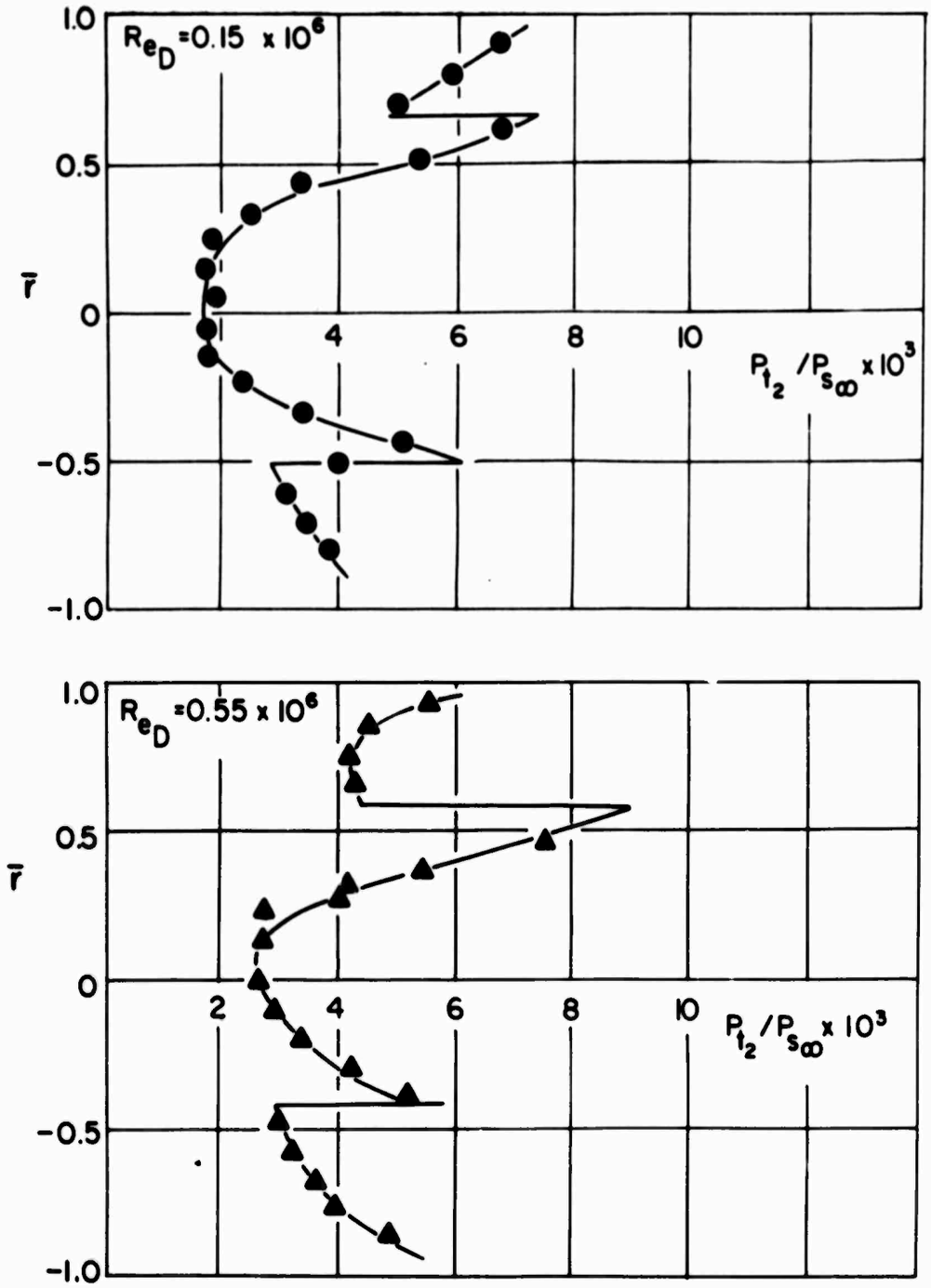

FIG.(10) PITOT PRESSURE PROFILES
(e) $\bar{X}$ =3.80

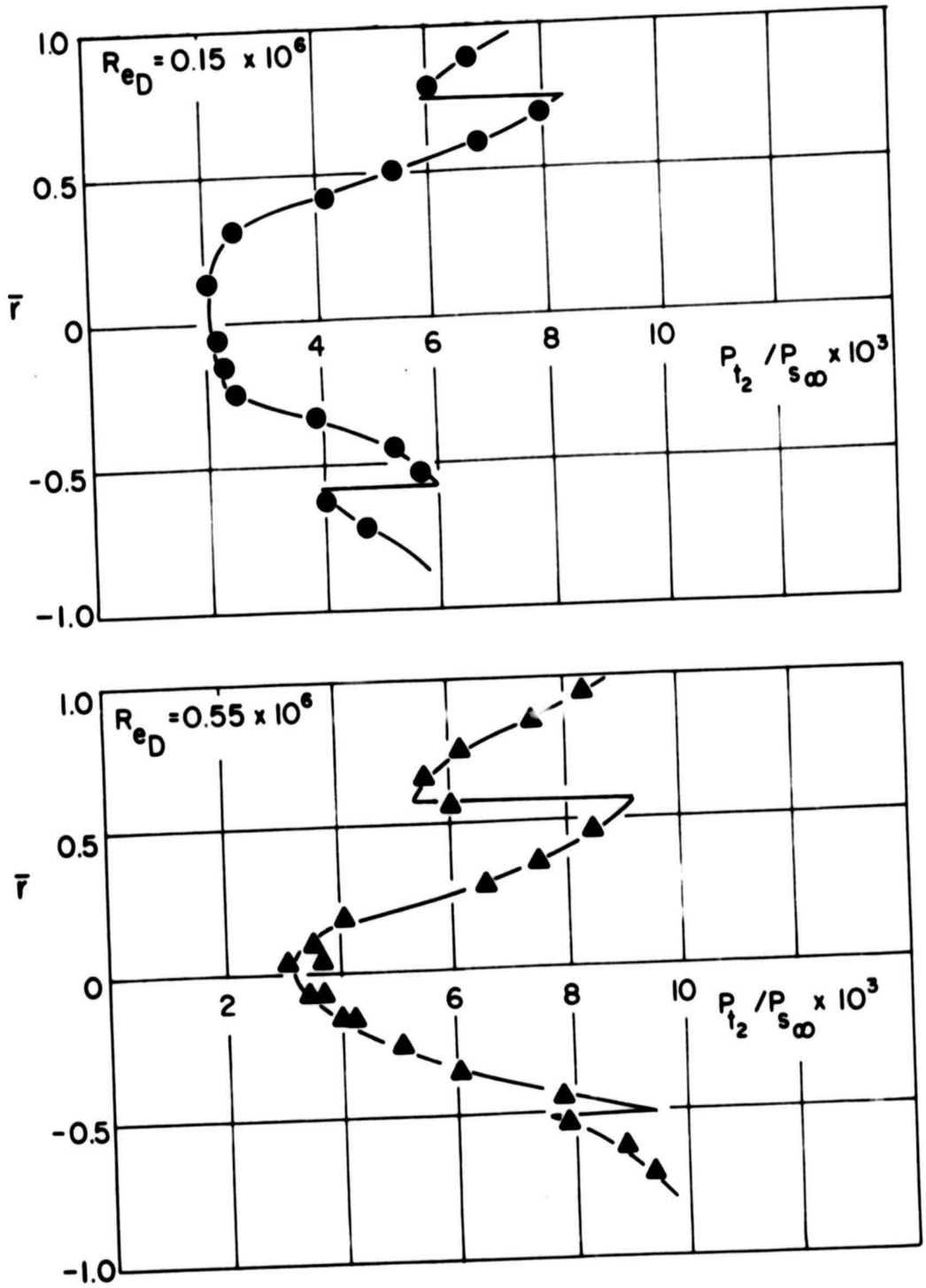

FIG.(10) PITOT PRESSURE PROFILES
(f) $\bar{X} = 4.50$

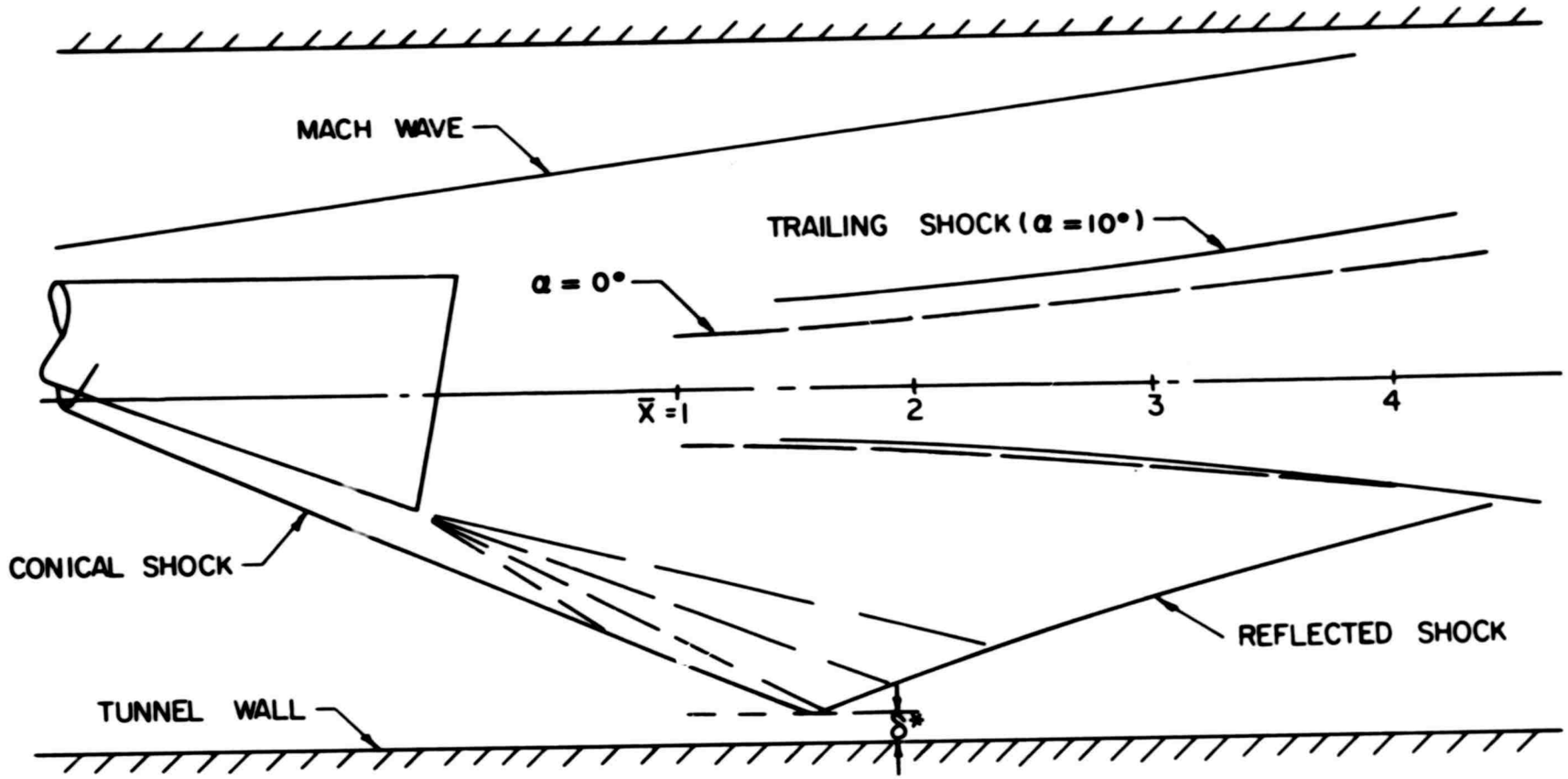

FIG. (11) SHOCK CONFIGURATION

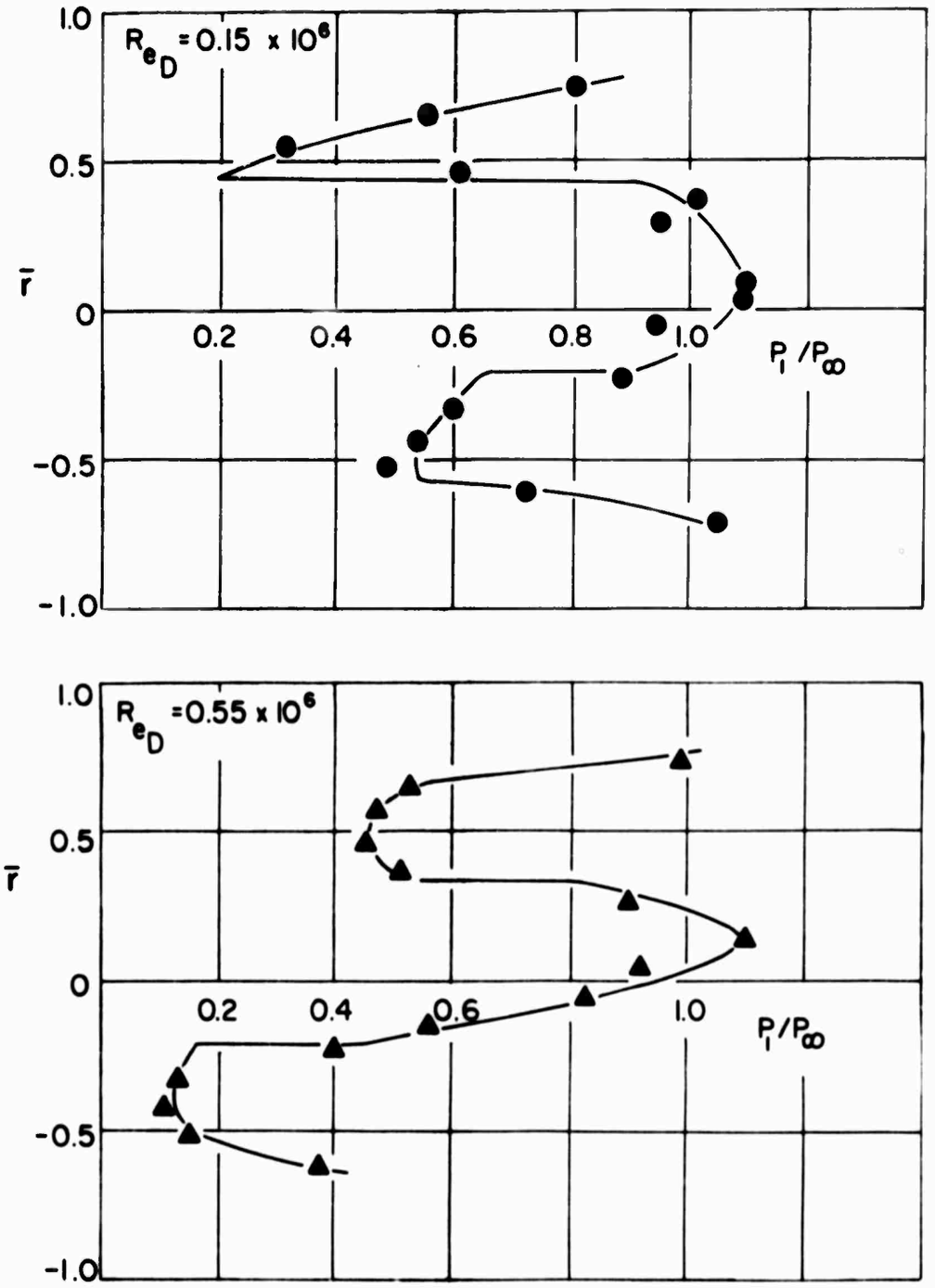

FIG. (12) STATIC PRESSURE PROFILES
(a) $\bar{X} = 1.50$

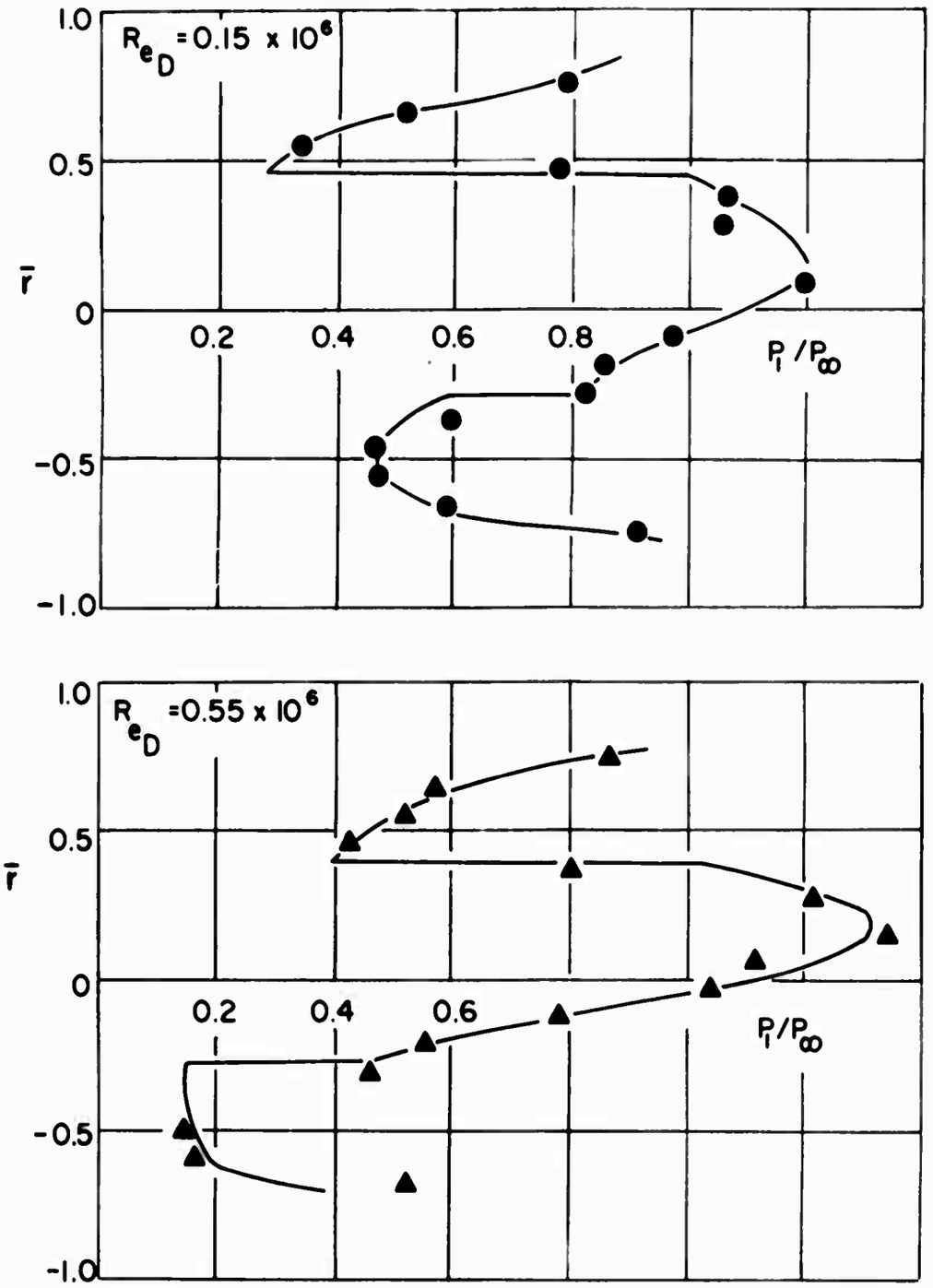

FIG. (12) STATIC PRESSURE PROFILES
(b) $\bar{X} = 2.00$

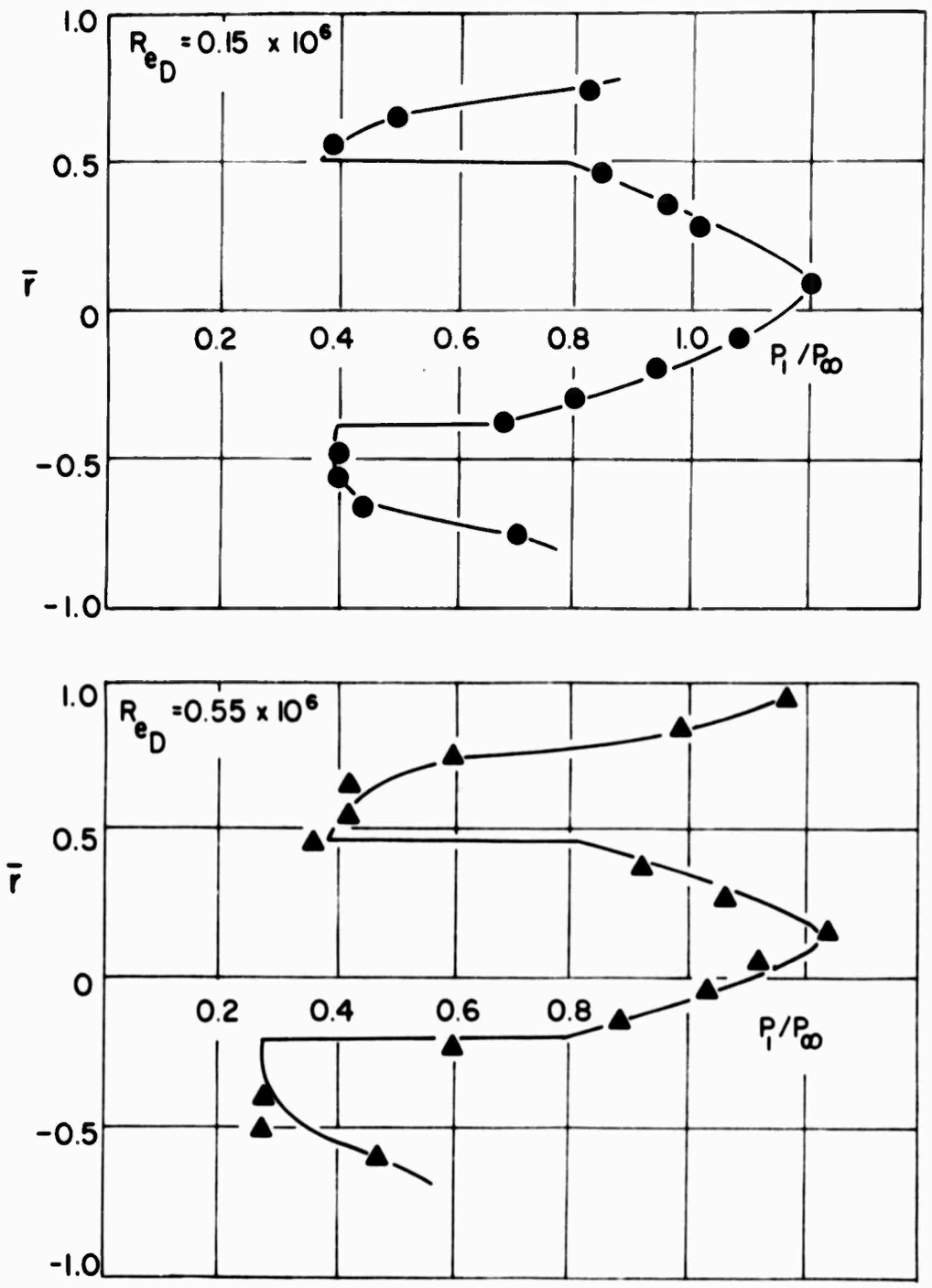

FIG. (12) STATIC PRESSURE PROFILES
(c) $\bar{X}$ = 2.50

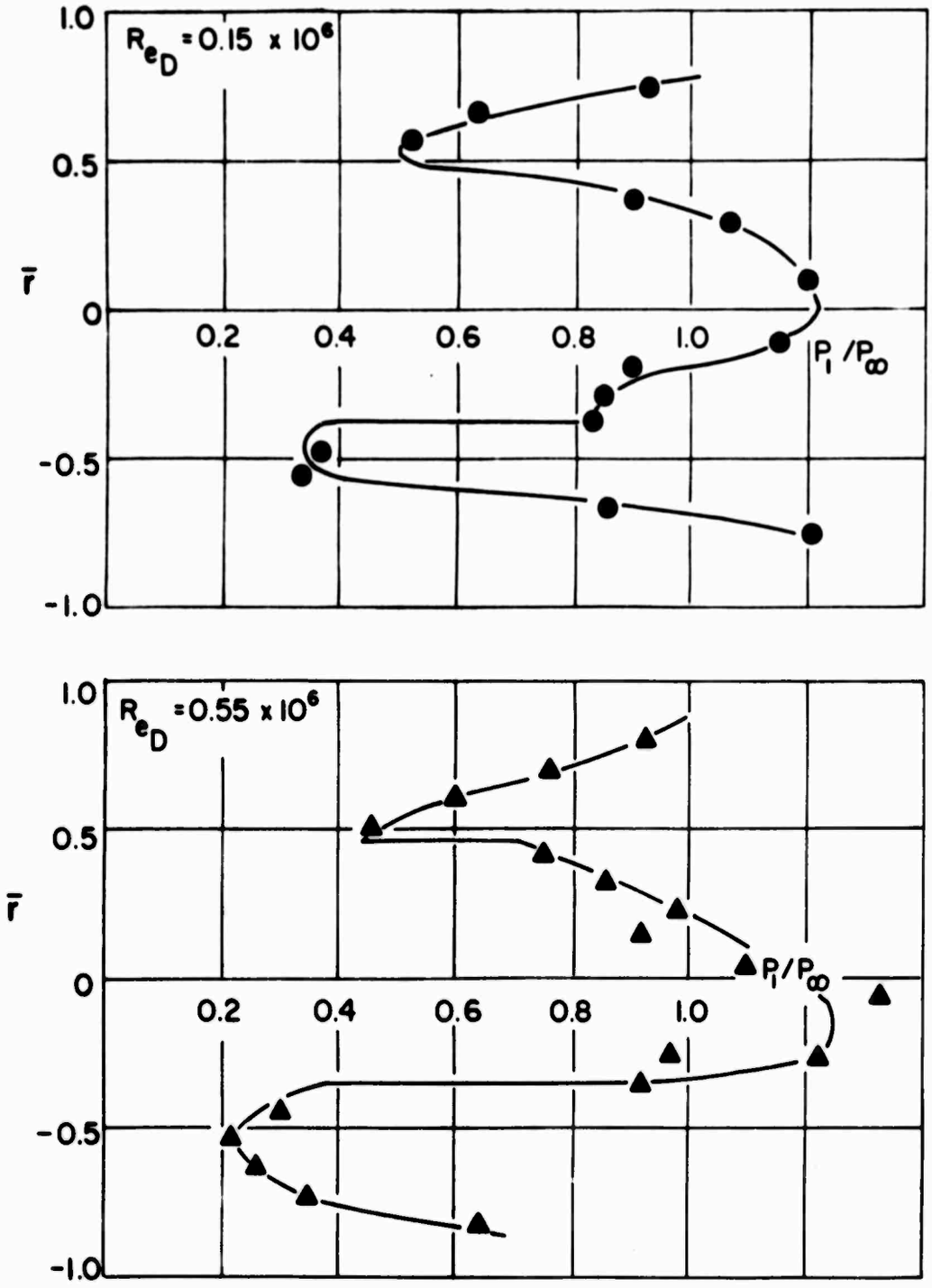

FIG. (12) STATIC PRESSURE PROFILES
(d) $\bar{X}$ = 3.00

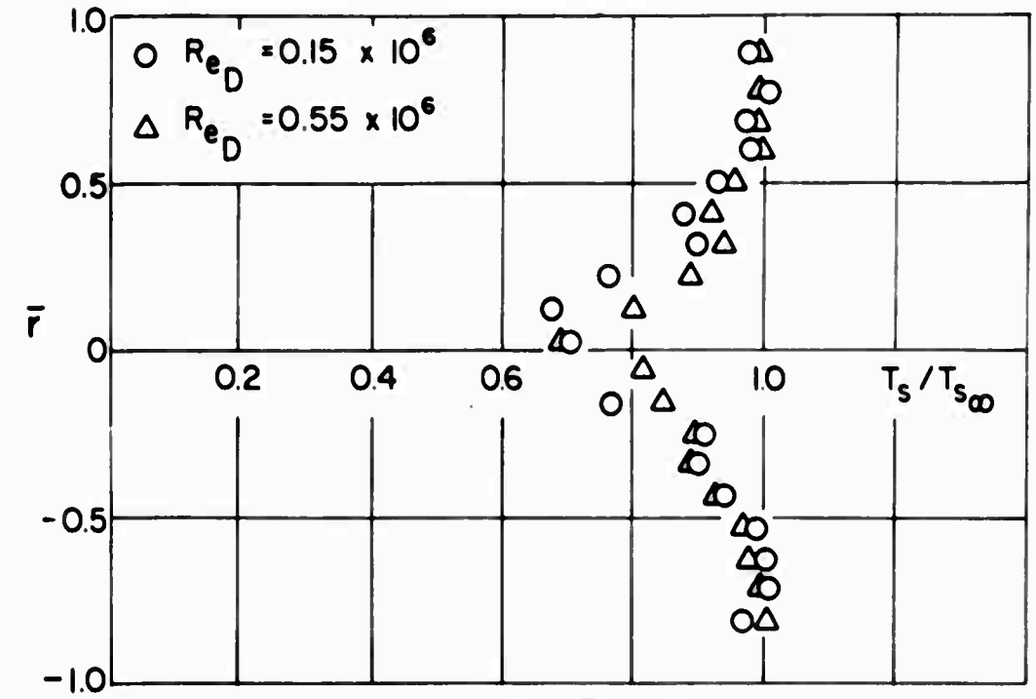

(a) $\bar{X}$ = 1.75

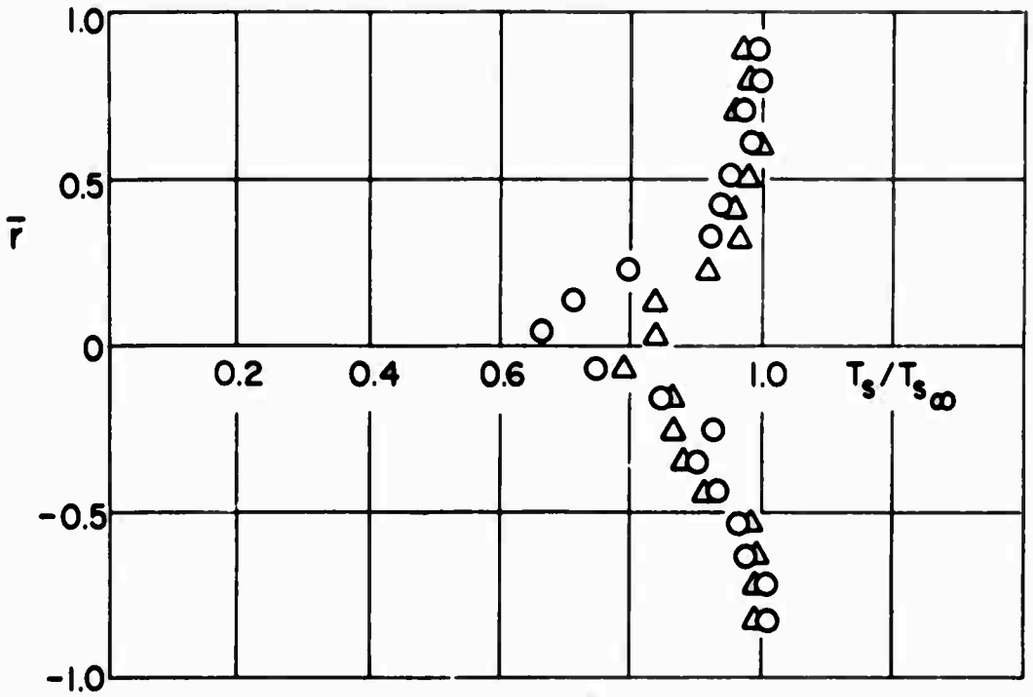

(b) $\bar{X}$ = 2.00

FIG. (13) STAGNATION TEMPERATURE PROFILES

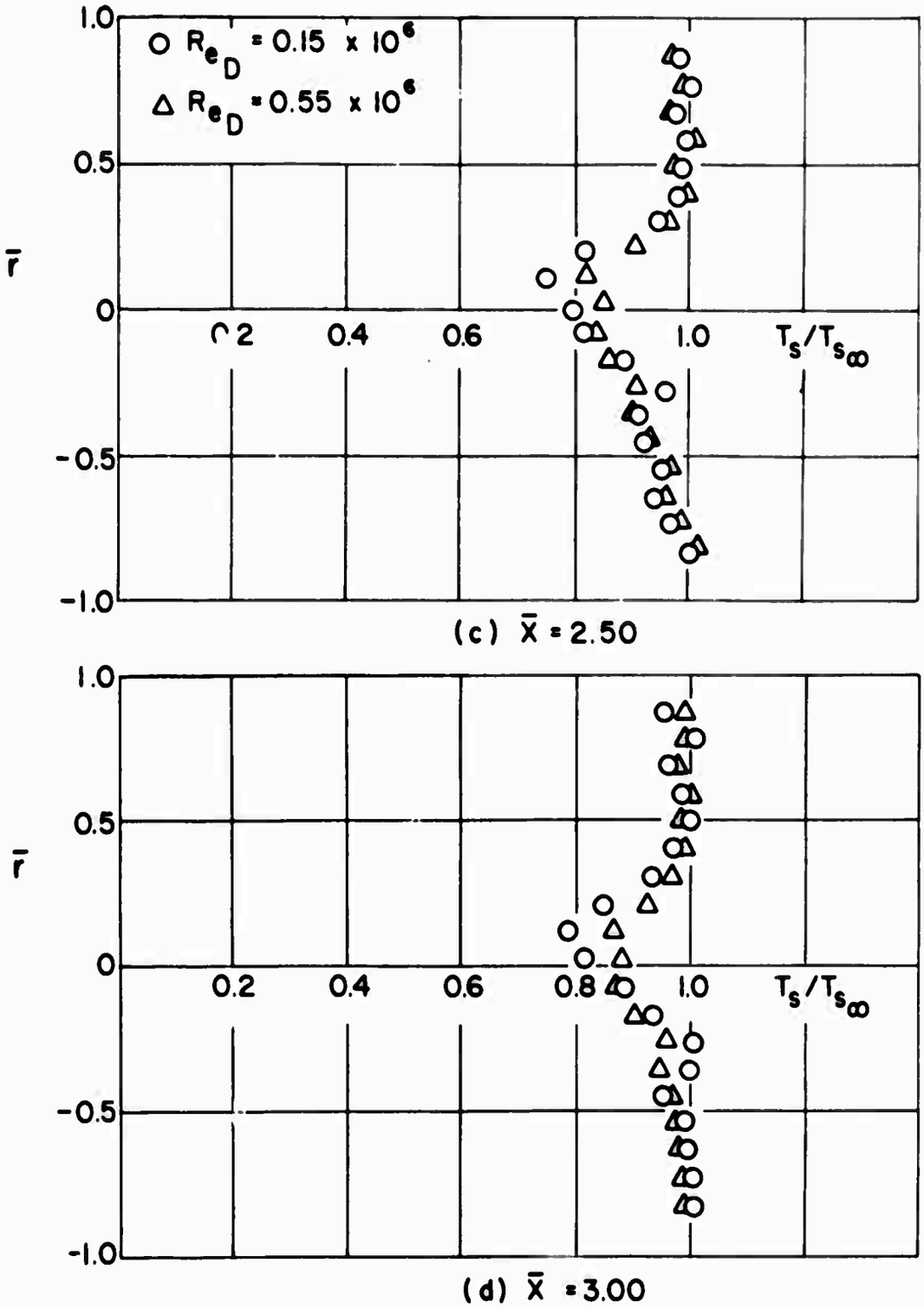

FIG. (13) STAGNATION TEMPERATURE PROFILES

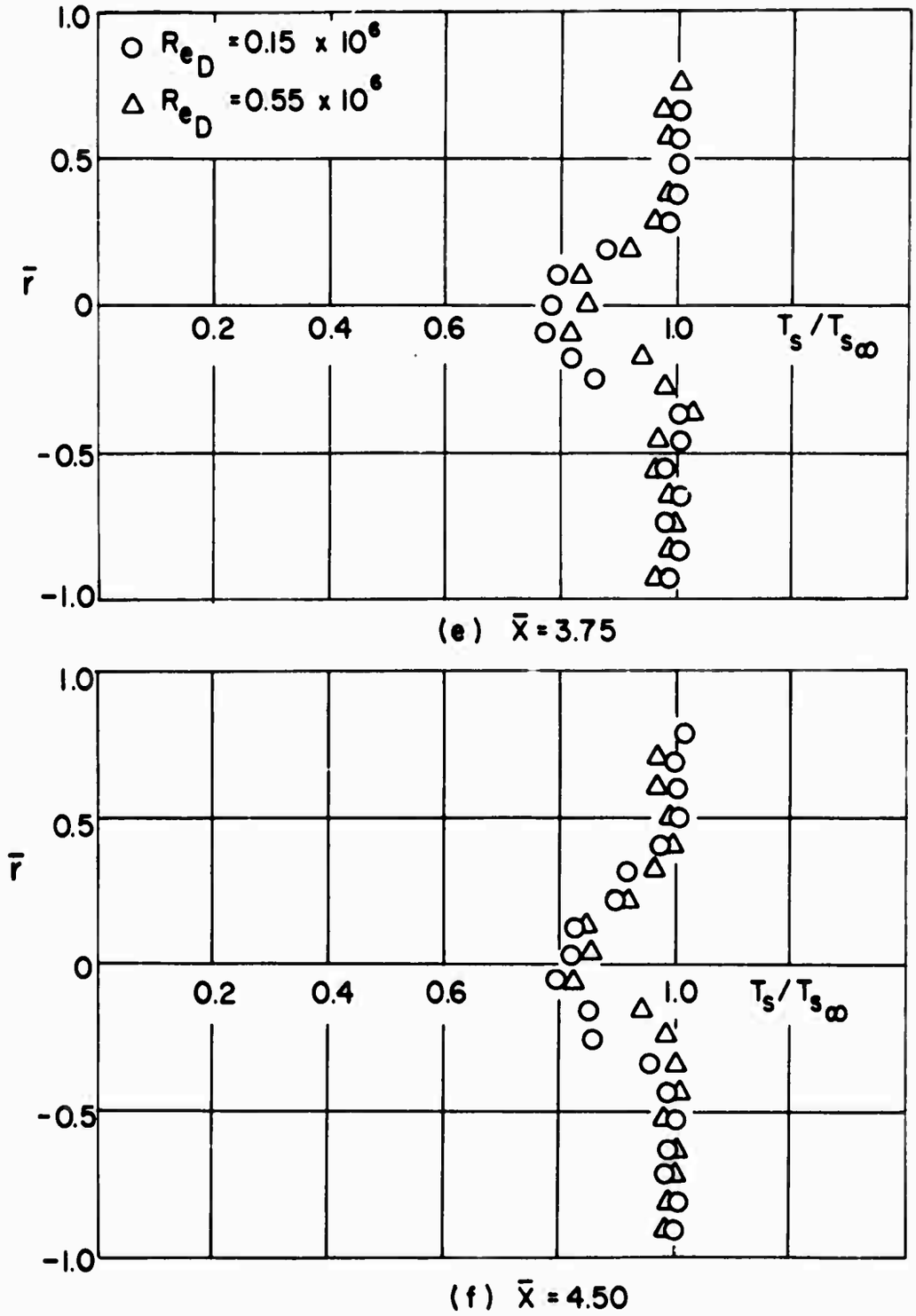

FIG. (13) STAGNATION TEMPERATURE PROFILES

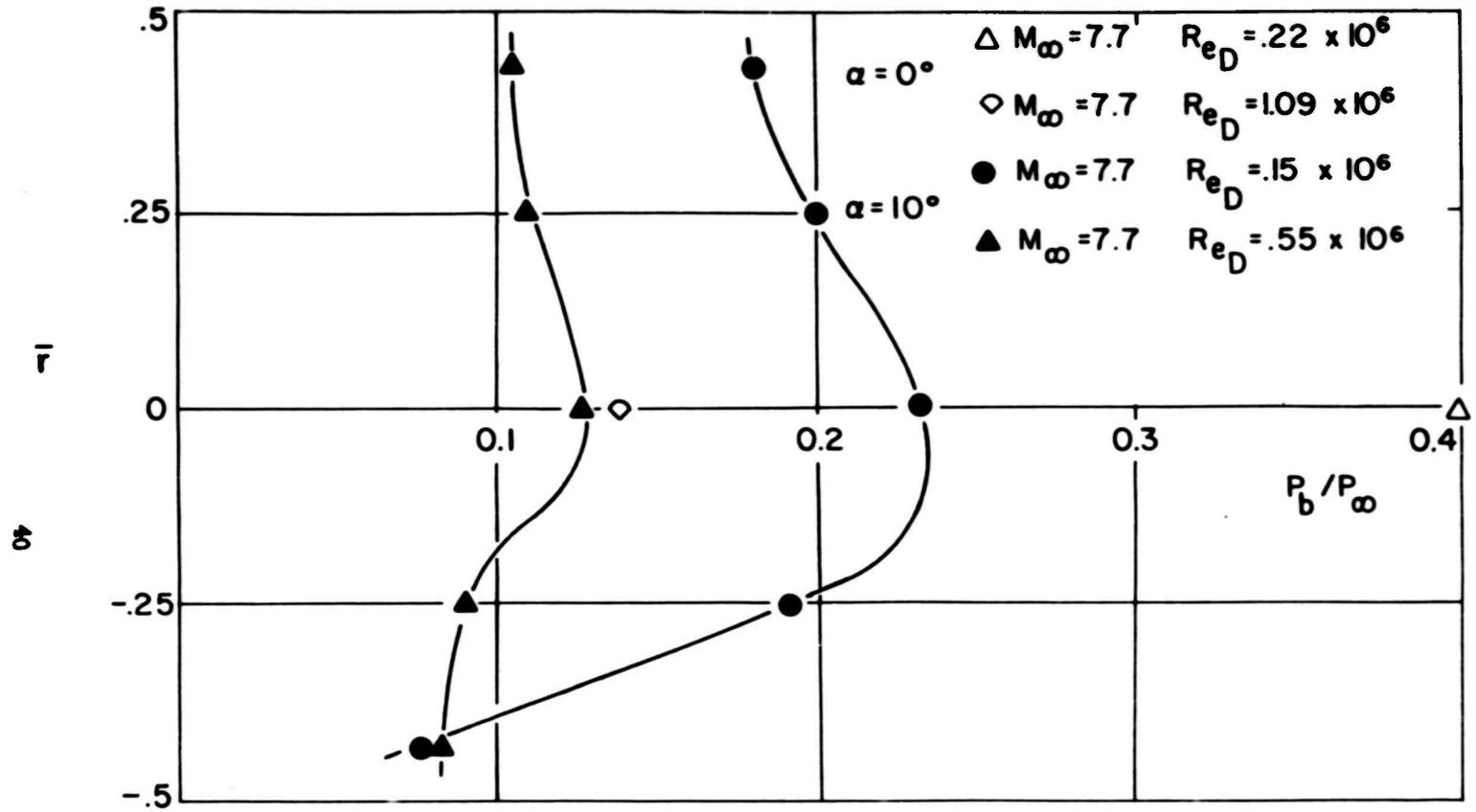

FIG. (14) BASE PRESSURE DISTRIBUTION

Unclassified

Security Classification

DOCUMENT CONTROL DATA - R & D

(Security classification of title, body of abstract and indexing annotation must be entered when the overall report is classified)

1. ORIGINATING ACTIVITY *(Corporate author)*

Polytechnic Institute of Brooklyn
Dept. of Aerospace Engrg. and Applied Mechanics
Route 110, Farmingdale, New York 11735

2a. REPORT SECURITY CLASSIFICATION

Unclassified

2b. GROUP

3. REPORT TITLE

NEAR WAKE OF A SLENDER CONE AT LARGE ANGLE OF ATTACK

4. DESCRIPTIVE NOTES *(Type of report and inclusive dates)*

Research Report

5. AUTHOR(S) *(First name, middle initial, last name)*

E. M. Schmidt and Robert J. Cresci

6. REPORT DATE

July 1968

7a. TOTAL NO. OF PAGES

40

7b. NO. OF REFS

14

8a. CONTRACT OR GRANT NO.

Nonr 839(38)

b. PROJECT NO.

c. ARPA Order No. 529

d.

9a. ORIGINATOR'S REPORT NUMBER(S)

PIBAL Report No. 68-23

9b. OTHER REPORT NO(S) *(Any other numbers that may be assigned this report)*

10. DISTRIBUTION STATEMENT

Distribution of this document is unlimited.

11. SUPPLEMENTARY NOTES

12. SPONSORING MILITARY ACTIVITY

Office of Naval Research
Department of the Navy
Washington, D.C.

13. ABSTRACT

The near wake of a sharp, slender cone at an angle of attack equal to the half-cone angle (10°) is studied experimentally. Tests were run at two different Reynolds numbers; these correspond to (i) completely laminar flow on the surface ($Re_D = 0.15 \times 10^6$) and, (ii) laminar flow on the windward and turbulent on the leeward surface ($Re_D = 0.55 \times 10^6$). The nature of the surface boundary layer was determined by measuring the surface heat transfer over a wide range of test Reynolds numbers ($0.6 \times 10^5 \leq Re_D \leq 1.2 \times 10^6$) and comparing the data with theoretical analyses.

Wake data obtained correspond to radial profiles taken in the plane of symmetry; total temperature, pitot, and static pressures are measured from the rear stagnation point to approximately seven diameters downstream of the base. Centerline distributions of Mach number, stagnation pressure, and static temperature are computed and compared to the corresponding results at zero angle of attack.

DD FORM 1 NOV 65 1473

Unclassified

Security Classification

14 KEY WORDS	LINK A ROLE	LINK A WT	LINK B ROLE	LINK B WT	LINK C ROLE	LINK C WT
Hypersonic wake						
Flow measurements						
Conical flow						